IRX1 hypomethylation promotes osteosarcoma metastasis via induction of CXCL14/NF-κB signaling

Jinchang Lu,[1] Guohui Song,[1] Qinglian Tang,[1] Changye Zou,[1] Feng Han,[2] Zhiqiang Zhao,[1] Bicheng Yong,[1,3] Junqiang Yin,[1] Huaiyuan Xu,[1] Xianbiao Xie,[1] Tiebang Kang,[4] YingLee Lam,[2] Huiling Yang,[5] Jingnan Shen,[1] and Jin Wang[1]

[1]Department of Musculoskeletal Oncology, the First Affiliated Hospital of Sun Yat-Sen University, Guangzhou, Guangdong, China. [2]Division of General Orthopaedics and Oncology, Department of Orthopaedics and Traumatology, University of Hong Kong, Queen Mary Hospital, Hong Kong, China. [3]Department of Pediatric Orthopedics, Guangzhou Women and Children's Hospital, Guangzhou, Guangdong, China. [4]State Key Laboratory of Oncology in South China, Sun Yat-Sen University Cancer Center, Guangzhou, China. [5]Department of Pathophysiology, Zhongshan School of Medicine, Sun Yat-Sen University, Guangzhou, Guangdong, China.

Osteosarcoma is a common malignant bone tumor with a propensity to metastasize to the lungs. Epigenetic abnormalities have been demonstrated to underlie osteosarcoma development; however, the epigenetic mechanisms that are involved in metastasis are not yet clear. Here, we analyzed 2 syngeneic primary human osteosarcoma cell lines that exhibit disparate metastatic potential for differences in epigenetic modifications and expression. Using methylated DNA immunoprecipitation (MeDIP) and microarray expression analysis to screen for metastasis-associated genes, we identified Iroquois homeobox 1 (*IRX1*). In both human osteosarcoma cell lines and clinical osteosarcoma tissues, *IRX1* overexpression was strongly associated with hypomethylation of its own promoter. Furthermore, experimental modulation of IRX1 in osteosarcoma cell lines profoundly altered metastatic activity, including migration, invasion, and resistance to anoikis in vitro, and influenced lung metastasis in murine models. These prometastatic effects of IRX1 were mediated by upregulation of CXCL14/NF-κB signaling. In serum from osteosarcoma patients, the presence of *IRX1* hypomethylation in circulating tumor DNA reduced lung metastasis–free survival. Together, these results identify *IRX1* as a prometastatic gene, implicate *IRX1* hypomethylation as a potential molecular marker for lung metastasis, and suggest that epigenetic reversion of *IRX1* activation may be beneficial for controlling osteosarcoma metastasis.

Introduction

Osteosarcoma, the most common primary malignant bone tumor, occurs most frequently in children and adolescents and has a strong tendency to metastasize. Pulmonary metastasis is the main cause of medical therapy failure and death in osteosarcoma patients. Despite an intensive search for new therapeutic strategies, survival has not improved over the past 2 decades (1). Given that controlling metastasis is the key to improving survival, there is an urgent need to investigate the underlying mechanisms of osteosarcoma metastasis and to develop more effective approaches to suppress lung metastasis.

It is widely accepted that the multistep process of cancer evolution is driven by both genetic and epigenetic abnormalities (2). Unlike genetic alterations, epigenetic changes are potentially reversible, making them attractive and promising targets for therapeutic intervention. Previous studies indicated that abnormal DNA methylation, a major epigenetic modification, is involved in the dysregulation of the cell cycle and apoptosis as well as in the proliferation and differentiation of osteosarcoma (3, 4). However, the epigenetic mechanisms of osteosarcoma metastasis remain largely unknown.

Iroquois homeobox 1 (IRX1), a member of the Iroquois homeobox family of transcription factors, plays a crucial role in embryonic development (5). Recently, *IRX1* was identified as a potential tumor-suppressor gene in head and neck squamous cell carcinoma (HNSCC) and gastric cancer (6, 7); however, further efforts are required to determine the exact function of IRX1 in the development of other cancers, including osteosarcoma. IRX1 is involved in limb development (8) and the etiology of kyphoscoliosis (9), suggesting that aberrant IRX1 expression may contribute to abnormal bone formation. Moreover, a gain of chromosome 5p15.33 (chromosomal location of *IRX1*) has been frequently detected in osteosarcoma cell lines (10). Therefore, the role of IRX1 in the pathogenesis of osteosarcoma is of interest.

Chemokine (C-X-C motif) ligand 14 (CXCL14), also known as BRAK, is a small cytokine belonging to the CXC chemokine family (11), and the gene encoding CXCL14 is commonly recognized as a tumor-suppressor gene (12–14). However, recent studies indicated that CXCL14 might actually promote tumor progression in some types of cancer (15–18). For example, CXCL14 was upregulated in pancreatic cancer tissues and enhanced the invasiveness of pancreatic cancer cells (17). *CXCL14* transcript levels are markedly high in papillary thyroid carcinoma and are positively correlated with lymph node metastasis (16). We previously showed that overexpression of CXCL14 predicts poor overall survival in osteosarcoma patients (19); however, its biological function in osteosarcoma metastasis requires further assessment.

Authorship note: Jinchang Lu, Guohui Song, and Qinglian Tang contributed equally to this work.
Conflict of interest: The authors have declared that no conflict of interest exists.
Submitted: August 8, 2014; **Accepted:** February 19, 2015.
Reference information: *J Clin Invest*. 2015;125(5):1839–1856. doi:10.1172/JCI78437.

Here, we used high-throughput approaches to identify novel epigenetically regulated metastasis-related genes in osteosarcoma. We found that IRX1 is epigenetically activated in highly metastatic osteosarcoma cell lines. IRX1 expression in primary human osteosarcoma samples was positively associated with promoter hypomethylation. The downregulation of IRX1 in osteosarcoma cell lines resulted in decreased CXCL14 expression levels, inhibition of NF-κB activity, and suppression of metastasis. Moreover, the hypomethylation of *IRX1* in serum from patients was correlated with a high risk of lung metastasis. Taken together, our findings represent a significant step forward in understanding the role of the epigenetically activated gene *IRX1* in osteosarcoma metastasis and provide a potential target for epigenetic-based osteosarcoma therapy.

Results

Epigenetic screen for genes driving invasion and metastasis in osteosarcoma. We previously established 2 syngeneic human osteosarcoma cell lines, ZOS and ZOSM, which were derived from a primary tumor and a skip metastasis, respectively, in the same patient (20). Biologically, ZOSM cells are more invasive and metastatic than are ZOS cells. To explore the underlying epigenetic mechanisms related to metastasis, we performed a methylated DNA immunoprecipitation (MeDIP) assay in combination with expression profiling using these 2 primary cell lines. MeDIP and expression array data were then filtered and integrated. Compared with ZOS, 18 genes showed promoter hypomethylation and were upregulated in ZOSM, while 8 genes exhibited promoter hypermethylation and were downregulated in ZOSM cells (Supplemental Table 1 and Figure 1A). Some of these upregulated genes, including *HOXB7*, *EpCAM*, and *CXCL6*, were previously reported to be involved in cancer metastasis. Notably, high expression levels of PRAME were recently found to be associated with poor prognosis and lung metastasis of human osteosarcoma in our previous study (21). The identification of these known metastasis-related genes suggested that our high-throughput platform was effective for the discovery of genes that drive osteosarcoma metastasis.

Therefore, using real-time PCR, we determined the expression levels of the 26 differentially expressed genes selected (listed in Figure 1A). Among these genes, our results demonstrated that the greatest difference in expression levels of *IRX1* was observed between ZOS and ZOSM cells (Supplemental Figure 1A). Therefore, we focused on IRX1 in this study, while other candidates such as *SALL1* were investigated in separate studies. On the basis of our real-time PCR results, there was a greater than 15-fold increase in *IRX1* expression in highly metastatic ZOSM cells compared with that detected in nonmetastatic ZOS cells (Figure 1B). To confirm that the *IRX1* expression pattern was not specific to only the primary cell lines, we examined *IRX1* expression levels in 2 other commonly used osteosarcoma cell lines, MNNG-HOS (poorly metastatic) and 143B (highly metastatic), both of which are derived from the TE85 human osteosarcoma cell line (22). As expected, higher *IRX1* mRNA expression was detected in the highly metastatic 143B cells relative to the mRNA levels in MNNG-HOS cells (Figure 1B). Accordingly, IRX1 protein levels were also substantially upregulated in ZOSM and 143B cells, as indicated by Western blot and immunofluorescence analyses (Figure 1C and Supplemental Figure 1B). We next examined *IRX1* mRNA expression levels in human osteosarcoma tissues and found that tissues from patients with lung metastasis showed higher *IRX1* expression levels than did tissues from patients without lung metastasis (Figure 1D). To further evaluate the clinical relevance of IRX1 in osteosarcoma metastasis, we collected 16 pairs of archival samples of osteosarcoma lung metastases and their corresponding primary osteosarcoma tissues. Immunohistochemical staining showed that the IRX1 expression scores were significantly higher in the lung metastases than in the primary tumors (Figure 1, E and F). These findings suggest that IRX1 plays an important role in osteosarcoma metastasis.

Elevated IRX1 expression is linked to hypomethylation of its own promoter. We next examined the association between IRX1 expression and its promoter methylation status in osteosarcoma. As shown in Figure 2A, a decreased methylation level was detected by bisulfite-sequencing PCR (BSP) in the promoter region of *IRX1* (–521 to –679 bp, which contains 5 predicted transcription factor–binding sites) in ZOSM and 143B cells compared with methylation levels detected in ZOS and MNNG-HOS cells (also see Supplemental Figure 2, A–C). Next, we analyzed *IRX1* promoter methylation levels in human osteosarcoma tissues. Genomic DNA isolated from 40 fresh surgical osteosarcoma specimens was treated with sodium bisulfite, amplified by PCR, and subjected to MassARRAY analysis. The results demonstrated that there was a significant correlation between increased *IRX1* expression and reduced promoter methylation (Figure 2, B and C). Furthermore, treatment of ZOS and MNNG-HOS cells with the methyltransferase inhibitor 5-aza-deoxycytidine (DAC), an effective DNA demethylating agent, significantly decreased the methylation level of the *IRX1* promoter and resulted in activation of *IRX1* gene expression (Figure 2, D and E, and Supplemental Figure 2D). Conversely, treatment of ZOSM and 143B cells with the methyl donor *S*-adenosyl-L-methionine (AdoMet), which has recently been shown to inhibit demethylase activity and induce DNA methylation (23), led to suppression of *IRX1* gene expression (Figure 2, F and G, and Supplemental Figure 2E).

To further explore whether DNA methylation directly regulates *IRX1* promoter activity, we cloned the promoter region of *IRX1* (–521 to –679 bp) into a luciferase reporter construct. The cloned fragment was methylated in vitro by *Sss*I methylase (methylation of 12 CpGs), HpaII methylase (methylation of 2 CpGs), or HhaI methylase (methylation of 2 CpGs). *IRX1* promoter activity was determined after transfection of 143B cells with methylated or mock-methylated luciferase constructs. As shown in Figure 2H, methylation repressed *IRX1* promoter activity in a methylation dose–dependent manner. Taken together, these results suggest that elevated IRX1 expression in osteosarcoma is associated with loss of methylation in the *IRX1* promoter.

IRX1 promotes the migration, invasion, and resistance to anoikis of osteosarcoma cells in vitro. Because osteosarcoma cells with a higher metastatic potential (ZOSM and 143B cells) exhibited elevated IRX1 expression (Figure 1, B and C), we sought to determine the role of IRX1 in osteosarcoma metastasis. It is well established that successful metastasis requires several essential steps. To evaluate the contribution of IRX1 to osteosarcoma cell migration, invasion, and resistance to anoikis in vitro, we

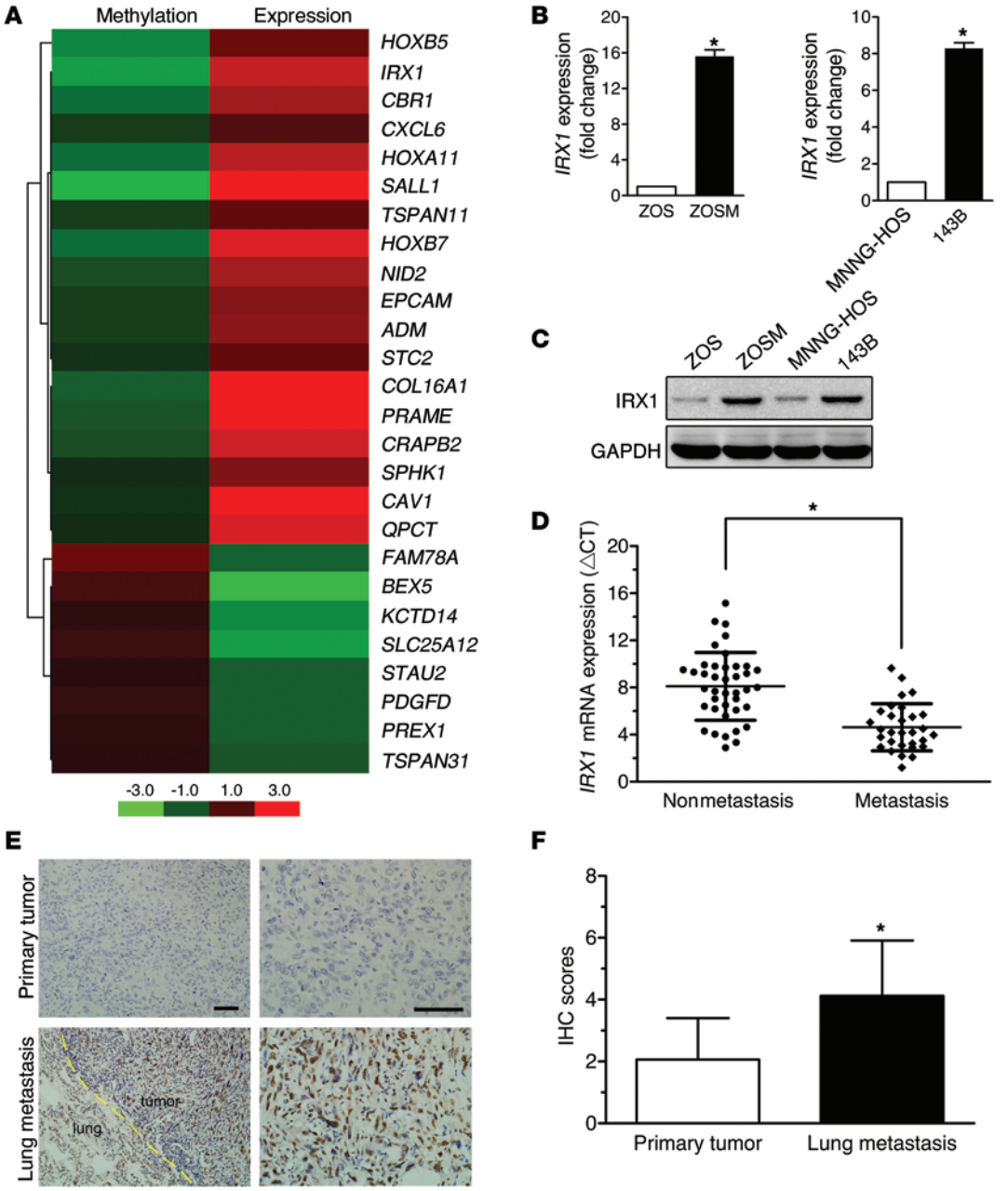

Figure 1. A high-throughput method to screen for epigenetically activated metastasis-driving genes in osteosarcoma. (**A**) Heatmap clustering of MeDIP and expression array data obtained from the 2 primary osteosarcoma cell lines ZOSM and ZOS. (**B**) Real-time PCR analysis. Data represent the mean ± SD of 3 separate determinations. (**C**) Western blot analysis. (**D**) *IRX1* mRNA expression in human osteosarcoma tissue (n = 70) was determined by real-time PCR. (**E**) Immunohistochemical staining of IRX1 in 16 pairs of primary osteosarcoma samples and their corresponding lung metastasis tissues. Scale bars: 100 μm. (**F**) Statistical analysis showed a significant increase in IRX1 expression in lung metastases relative to the expression in primary osteosarcoma samples. *P < 0.05 by Student's t test (**B** and **D**) and Wilcoxon signed-rank test (**F**).

first generated 2 lentiviral constructs encoding IRX1-targeting shRNAs and established cell lines in which IRX1 was stably knocked down (Figure 3A). We found that IRX1 knockdown did not influence cell proliferation (Supplemental Figure 3A). However, IRX1 downregulation inhibited the ability of ZOSM and 143B cells to fill the wound gap (Figure 3B) and migrate through Transwell membranes (Figure 3C). Suppression of IRX1 expression significantly reduced the invasive ability of both cell lines, as measured by Boyden chamber assays (Figure 3C). Given that anoikis is a physiological barrier to metastasis and that resistance to anoikis may facilitate distant organ metastasis (24, 25), we further examined the effect of IRX1 deletion on the anoikis of osteosarcoma cells by culturing cells on ultra-low attachment plates. After a 48-hour incubation, we found that ZOSM-shIRX1 and 143B-shIRX1 cells were more sensitive to detachment-induced apoptosis than were their scrambled controls (Figure 3D). These results suggest that IRX1 regulates the metastatic behavior of osteosarcoma cells.

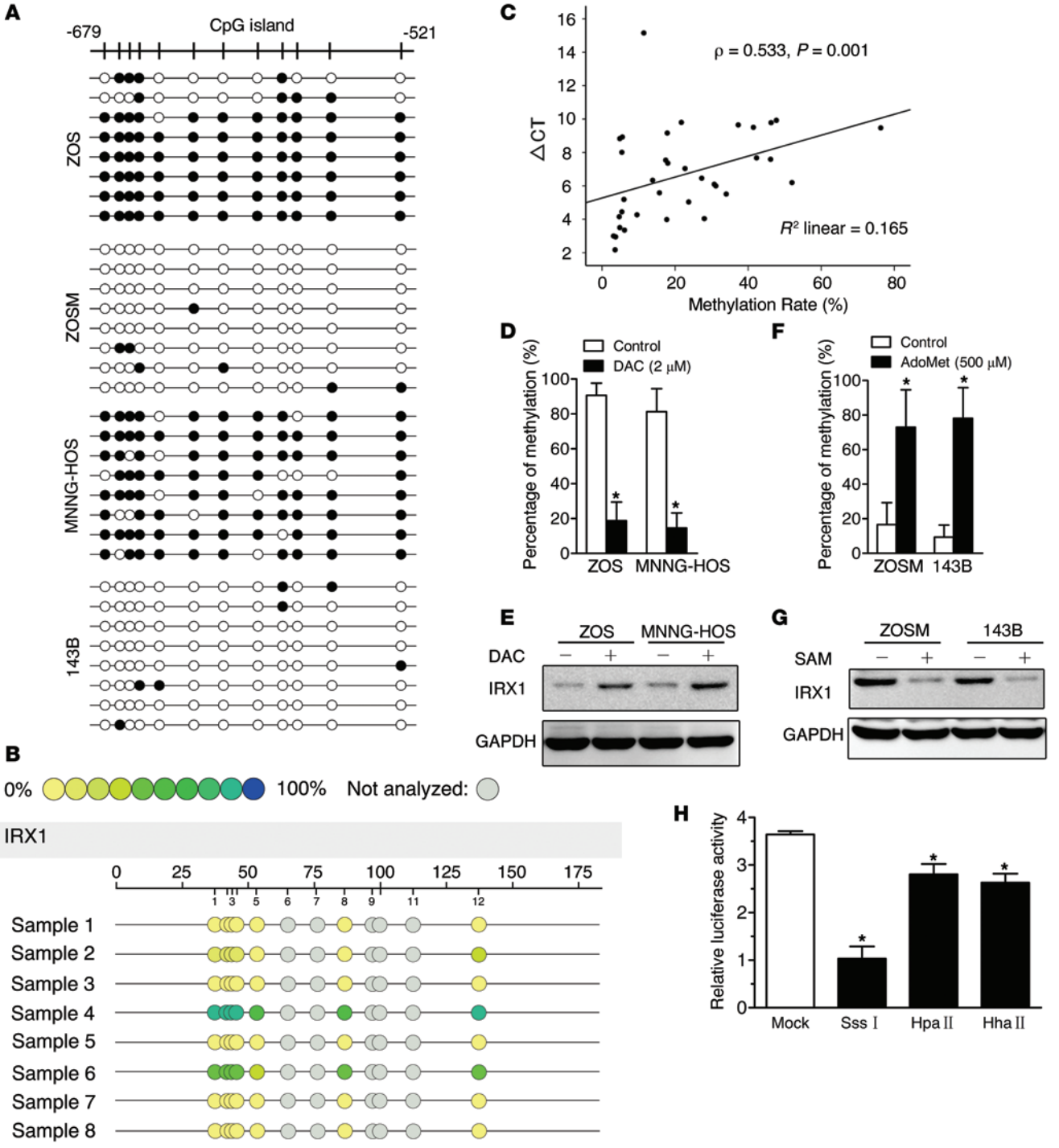

Figure 2. Elevated *IRX1* expression is associated with hypomethylation of its promoter. (**A**) BSP analysis of the *IRX1* promoter (–521 to –679) in 4 osteosarcoma cell lines. (**B**) Sequenom MassARRAY analysis of the *IRX1* promoter in 40 human osteosarcoma tissues. Data shown are from 8 representative samples. (**C**) *IRX1* expression was associated with a low methylation rate. $P = 0.001$ by Spearman's rank correlation analysis. (**D**) BSP analysis of the *IRX1* promoter in ZOS and MNNG/HOS cells after treatment with 2 μM DAC for 3 days. (**E**) Western blot analysis shows that treatment with 2 μM DAC induced IRX1 protein expression in ZOS and MNNG/HOS cells. (**F**) BSP analysis of the *IRX1* promoter in ZOSM and 143B cells after treatment with 500 μM AdoMet for 6 days. (**G**) Western blot analysis shows that treatment with 500 μM AdoMet suppressed IRX1 expression in ZOSM and 143B cells. (**H**) Methylated or mock-methylated *IRX1* promoter (–521 to –679) – luciferase reporter constructs were transiently transfected into 143B cells. Luciferase activity was analyzed after a 48-hour transfection. Values shown are the mean ± SD of 3 separate determinations. $^*P < 0.05$ by Student's *t* test (**D** and **F**) and 1-way ANOVA (**H**).

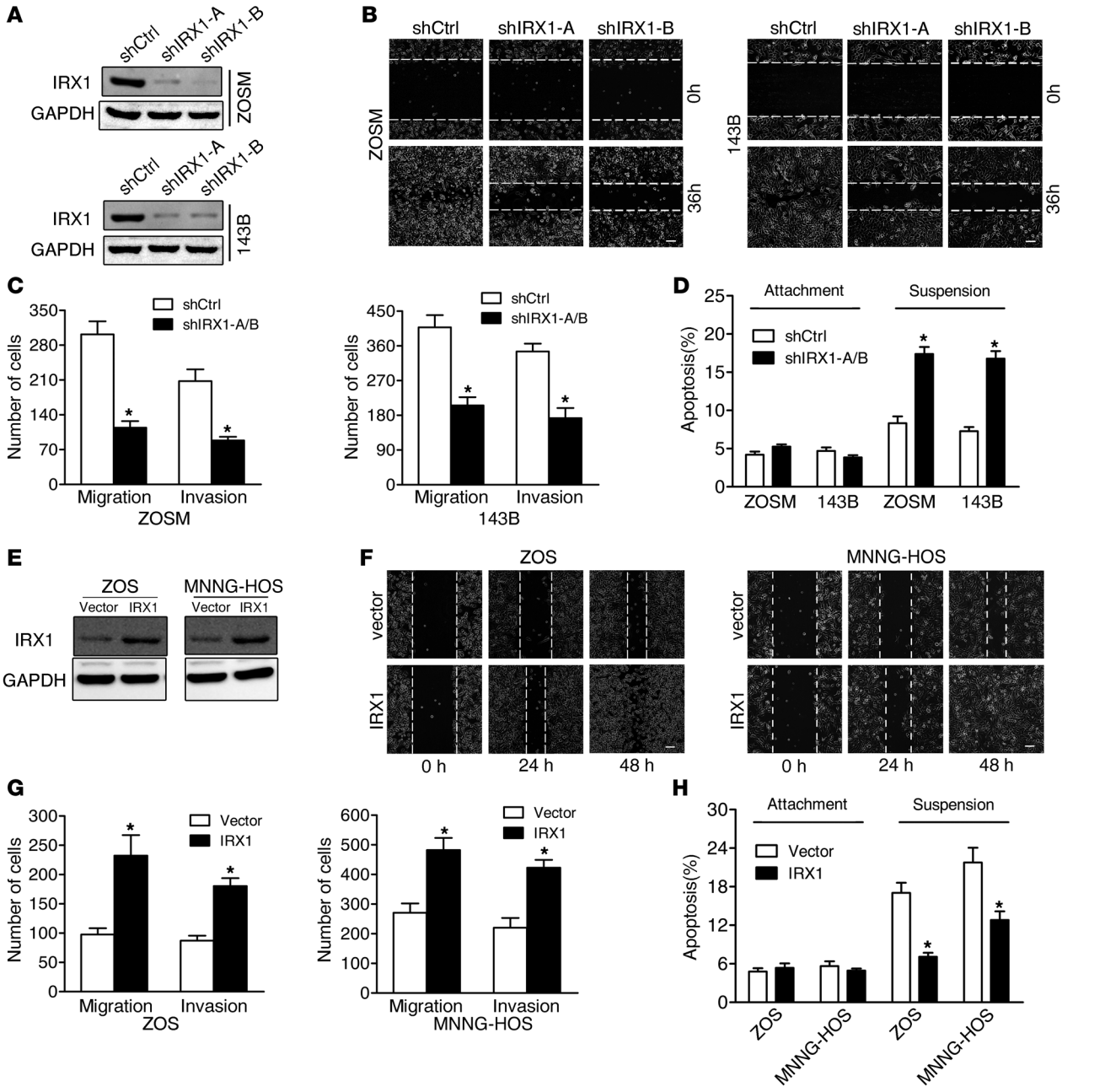

Figure 3. IRX1 promotes migration, invasion, and resistance to anoikis in osteosarcoma cells. (**A**) The effect of IRX1-targeting shRNAs was confirmed by Western blot analysis. (**B**) *IRX1* deletion dramatically reduced the migratory ability of osteosarcoma cells in a wound-healing assay. (**C**) Downregulation of IRX1 resulted in a decrease in the migratory and invasive abilities of osteosarcoma cells as determined by Transwell analysis. (**D**) FACS analysis indicated that IRX1 suppression significantly promoted the death of nonadherent cells but had no effect on attached cells. (**E**) The efficiency of IRX1 overexpression in ZOS and MNNG-HOS cells was confirmed by Western blot analysis. (**F**) IRX1 overexpression enhanced the migratory ability of osteosarcoma cells. (**G**) Overexpression of IRX1 in ZOS and MNNG-HOS cells increased their migratory and invasive abilities. (**H**) IRX1 overexpression inhibited cell death under nonadherent culture conditions. Data represent the mean ± SD of 3 separate determinations. Scale bars: 100 μm. $^*P < 0.05$ by Student's *t* test.

We further confirmed the positive effect of IRX1 on migration, invasion, and resistance to anoikis through gain-of-function studies. Here, we chose ZOS and MNNG-HOS cells that expressed low endogenous levels of IRX1 and exhibited weak metastatic ability. As expected, the ectopic overexpression of *IRX1* in ZOS and MNNG-HOS cells increased the migratory and invasive abilities of these cells, without influencing cell growth, and promoted anoikis resistance under suspension culture conditions (Figure 3, E–H, and Supplemental Figure 3B). Taken together, these results indicate that IRX1 positively regulates osteosarcoma cell migration, invasion, and resistance to anoikis.

IRX1 promotes osteosarcoma metastasis to the lung in vivo. We next examined the effect of IRX1 on osteosarcoma metastasis in vivo using mouse xenograft models. In our previous experimental metastasis assay, no metastases were found in mice injected with ZOS cells through the tail vein; however, mice injected with

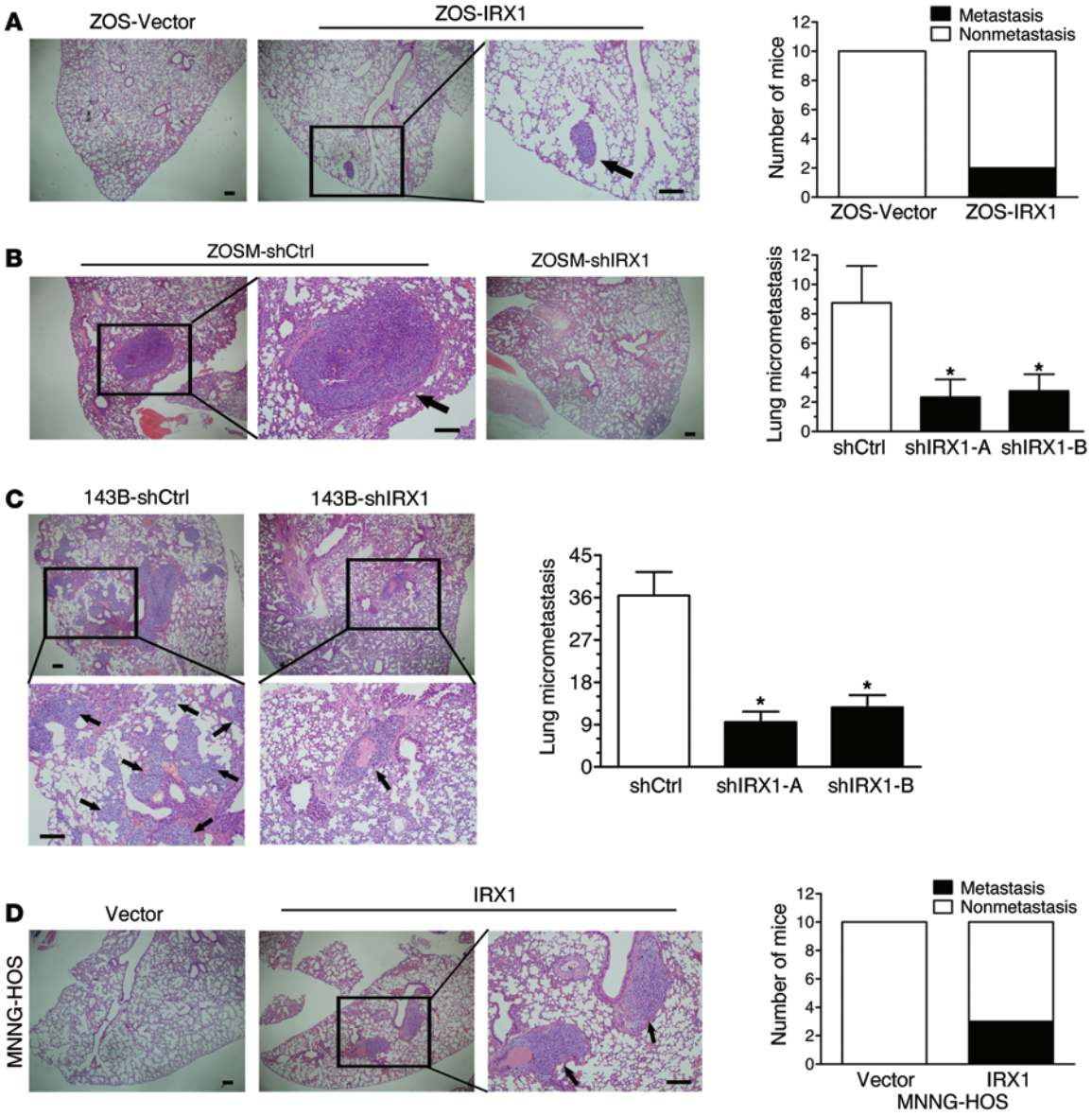

Figure 4. IRX1 promotes osteosarcoma metastasis to the lungs in a mouse model. (**A**) Overexpression of IRX1 increased the rate of lung metastasis after tail-vein injection of ZOS-IRX1 or control cells. (**B**) Suppression of IRX1 in ZOSM cells significantly decreased the number of lung metastases. (**C**) Mice bearing 143B-shControl (143B-shCtrl) cells developed multiple large metastases, while the suppression of IRX1 dramatically inhibited the lung metastasis of 143B cells. (**D**) IRX1 overexpression in poorly metastatic MNNG-HOS cells increased the metastatic rate in mice from 0% (0 of 10) to 30% (3 of 10). Representative histological images of lung sections are shown. Black arrow indicates the metastatic nodule. Scale bars: 200 μm. *$P < 0.05$ by Student's *t* test.

ZOSM cells developed pulmonary and spinal metastases (20). To determine whether IRX1 participates in establishing lung metastases, ZOS-IRX1, ZOSM-shIRX1-A/B, and their control cells were injected into the tail veins of NOD/SCID mice ($n = 10$ per group). After 8 weeks, we checked for lung micrometastases. None of the mice injected with ZOS control cells developed lung metastases, but 2 mice in the ZOS-IRX1 group developed small metastases in the lungs (Figure 4A). Meanwhile, IRX1 knockdown in ZOSM cells caused a significant reduction in lung metastasis (Figure 4B).

To better mimic the clinical scenario, we adopted an orthotopic mouse model to further explore the effect of IRX1 on osteosarcoma metastasis. 143B-shIRX1-A/B and control cells were injected into the proximal tibia of NOD/SCID mice ($n = 10$ per group), and tumor size was measured over time. After 5 weeks, the lungs were harvested, and micrometastases were analyzed. Consistent with the in vitro results, IRX1 knockdown in 143B cells did not affect primary tumor growth (Supplemental Figure 4, A–C), but markedly inhibited lung metastasis in vivo (Figure 4C). We then examined the effect of IRX1 overexpression in MNNG-HOS cells that rarely produced spontaneous lung metastases. While there was no significant difference in primary tumor growth between MNNG-HOS-IRX1 and control cells (Supplemental Figure 4, D and E), MNNG-HOS-IRX1 exhibited an increase in the rate of metastasis (from 0% to 30%), as shown in Figure 4D. Together, these findings confirm that IRX1 is involved in osteosarcoma lung metastasis in vivo.

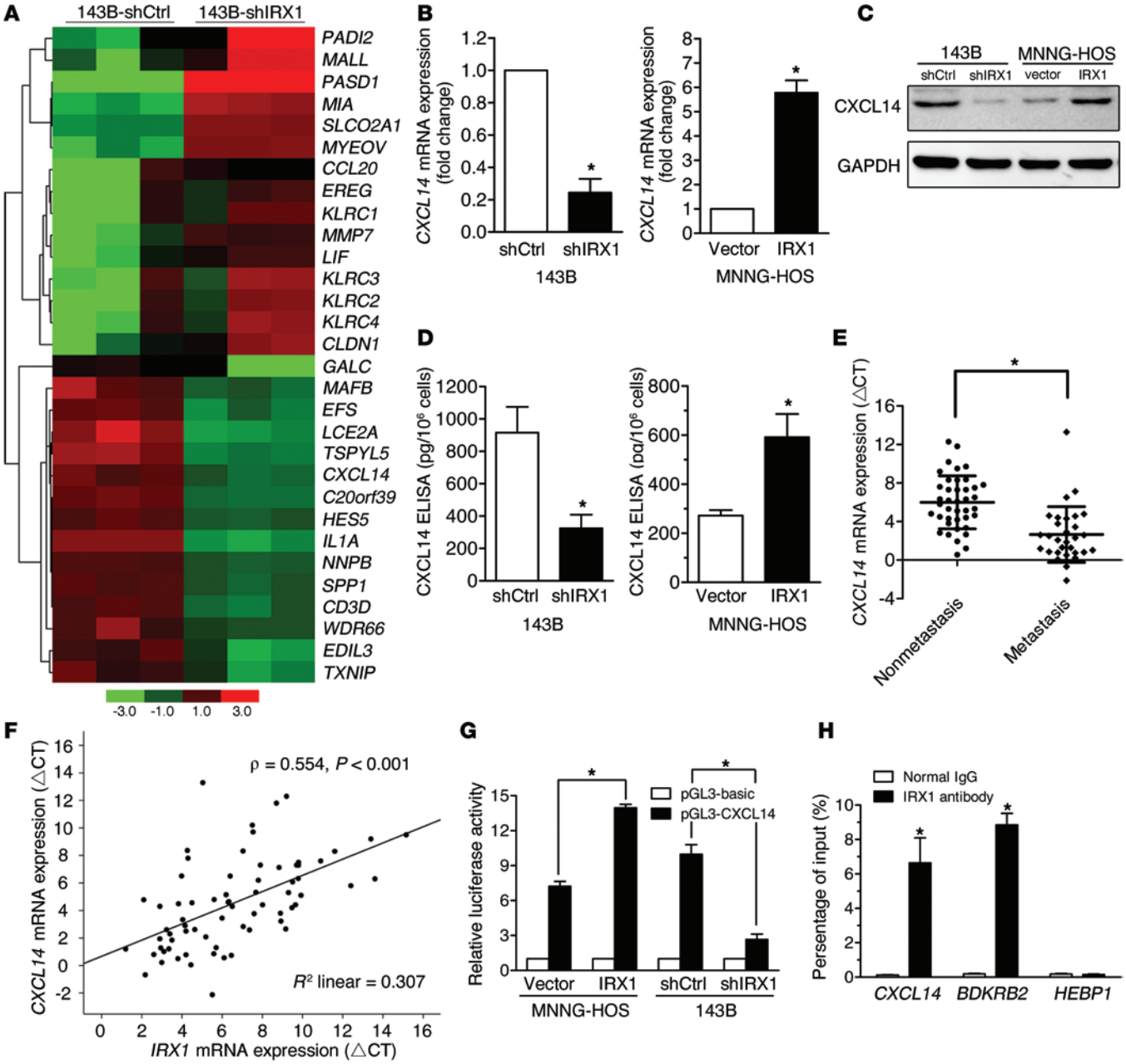

Figure 5. IRX1 expression upregulates *CXCL14* gene expression. (**A**) Microarray analysis demonstrated that IRX1 suppression led to decreased *CXCL14* mRNA levels in 143B cells. (**B**–**D**) *CXCL14* mRNA levels (**B**), CXCL14 protein expression (**C**), and secreted CXCL14 protein levels (**D**) were determined in 143B-shIRX1 and MNNG-HOS-IRX1 cells. (**E**) *CXCL14* mRNA expression levels in human osteosarcoma tissues (n = 70) were analyzed by real-time PCR. (**F**) *IRX1* expression was correlated with *CXCL14* expression in human osteosarcoma tissues (Pearson's correlation analysis, $P < 0.001$). (**G**) *CXCL14* promoter/luciferase reporter constructs (nucleotides –2000 to +515) were transiently transfected into the indicated cells, and luciferase activity was analyzed after 48 hours. (**H**) ChIP was performed to detect binding of IRX1 to the *CXCL14* promoter in 143B cells. PCR amplification result using the primers flanking site A (ACACCTGT) is shown (positive control: *BDKRB2*; negative control: *HEBP1*). Data represent the mean ± SD of 3 separate determinations. *$P < 0.05$ by Student's t test.

IRX1 upregulates CXCL14 expression. To explore the underlying mechanism by which IRX1 promotes osteosarcoma progression, we used a gene expression microarray to identify genes that were differentially expressed in 143B-shIRX1-A and control cells. A 2-fold screening filter was applied, and we found 115 upregulated genes and 78 downregulated genes in the 143B-shIRX1 cells relative to what was observed in the controls. The top 15 differentially expressed genes are shown in Supplemental Table 2 and Figure 5A; we mainly focused on genes with decreased expression after IRX1 knockdown. Among them, we were specifically interested in *CXCL14* (with an ~5-fold decrease), which has been reported to be associated with tumor progression and metastasis in select cancers (15, 17, 18). Importantly, our recent study demonstrated that CXCL14 expression was upregulated in osteosarcoma and predicted poor

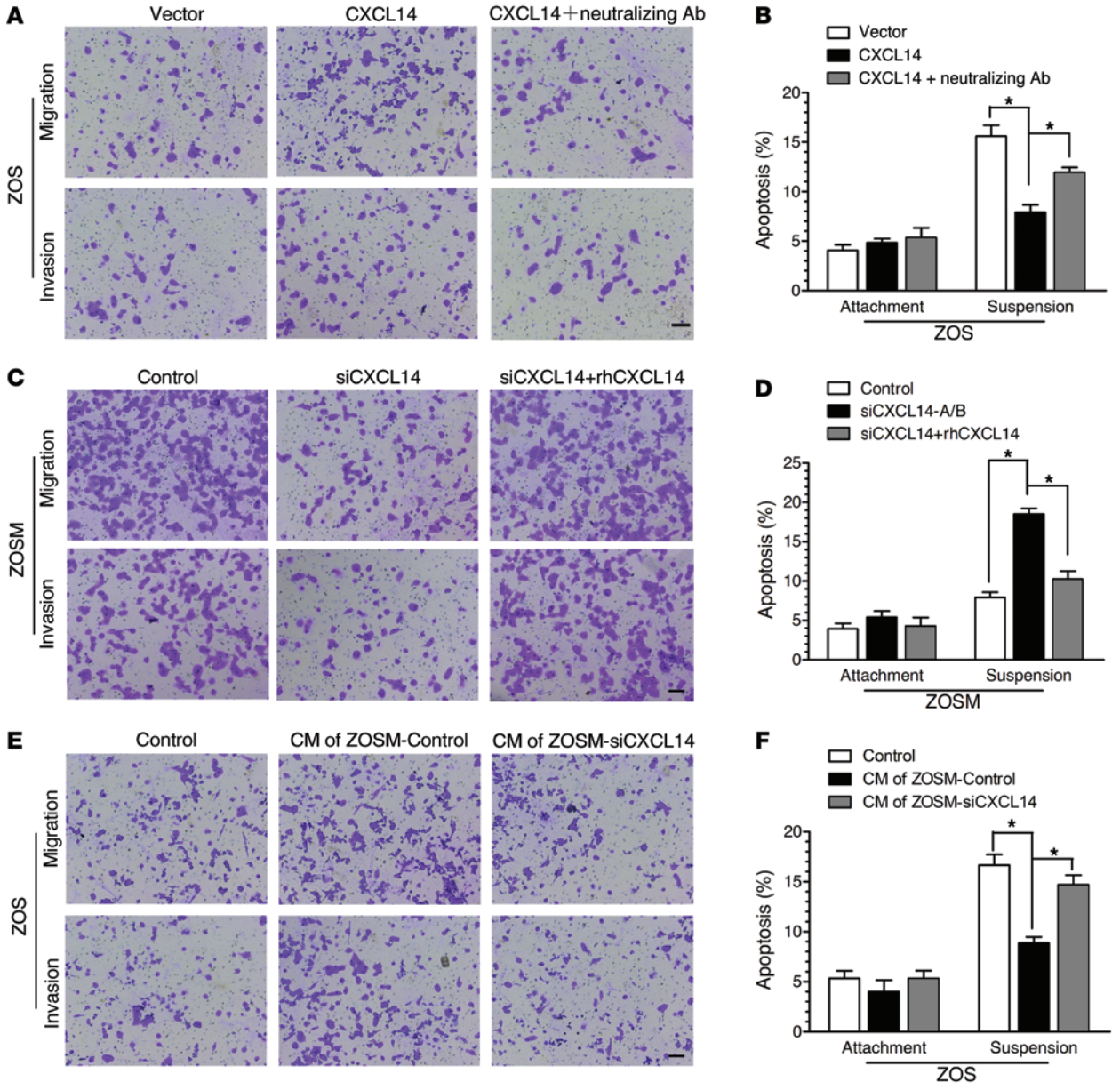

Figure 6. CXCL14 promotes the metastatic ability of osteosarcoma cells in an autocrine manner. (**A**) Transwell analysis of the indicated cells. CXCL14-neutralizing antibody (20 μg/ml) was used to block secreted CXCL14 in the culture medium of ZOS-CXCL14 cells. (**B**) The apoptotic rates of the indicated cells were determined by FACS analysis under attached and suspension conditions. (**C**) Transwell analysis of the indicated cells. Recombinant human CXCL14 (rhCXCL14, 200 ng/ml) was added to the culture medium of ZOSM-siCXCL14 cells. (**D**) Apoptotic rates of the indicated cells were determined by FACS. (**E**) Transwell analysis of ZOS cells cultured in conditioned medium (CM) from ZOSM control or ZOSM-siCXCL14 cells. (**F**) Apoptotic rates of the indicated cells were determined by FACS. Data represent the mean ± SD of 3 separate determinations. Scale bars: 100 μm. *$P < 0.05$ by Student's *t* test.

overall survival (19). Moreover, our cDNA microarray data showed that *CXCL14* mRNA transcription was markedly higher (33.9-fold) in the ZOSM cells (with high IRX1 expression) than in the ZOS cells (with low IRX1 expression). These results suggested that CXCL14 is a potential downstream target of IRX1 in osteosarcoma.

To confirm the microarray data, we examined the expression of CXCL14 in 143B-shIRX1 and MNNG-HOS-IRX1 cells using quantitative real-time PCR and Western blot analyses. CXCL14 mRNA and protein levels were downregulated by IRX1 shRNA transfection and upregulated by IRX1 overexpression (Figure 5, B and C). Moreover, we detected a decrease in secreted CXCL14 protein levels in the conditioned medium of 143B-shIRX1 cells, while we found increased levels of secreted CXCL14 protein in MNNG-HOS-IRX1 cells (Figure 5D). A similar IRX1-CXCL14 expression pattern was observed in ZOSM-shIRX1 and ZOS-IRX1 cells (Supplemental Figure 5). Next, we investigated the *CXCL14* mRNA expression pattern in osteosarcoma tissues. Higher *CXCL14* mRNA levels were found in patients with lung metastasis than in those without lung metastasis, and further analysis revealed that there was a positive correlation between *IRX1* and *CXCL14* expression (Figure 5, E and F). These results demonstrate that CXCL14 is positively regulated by IRX1.

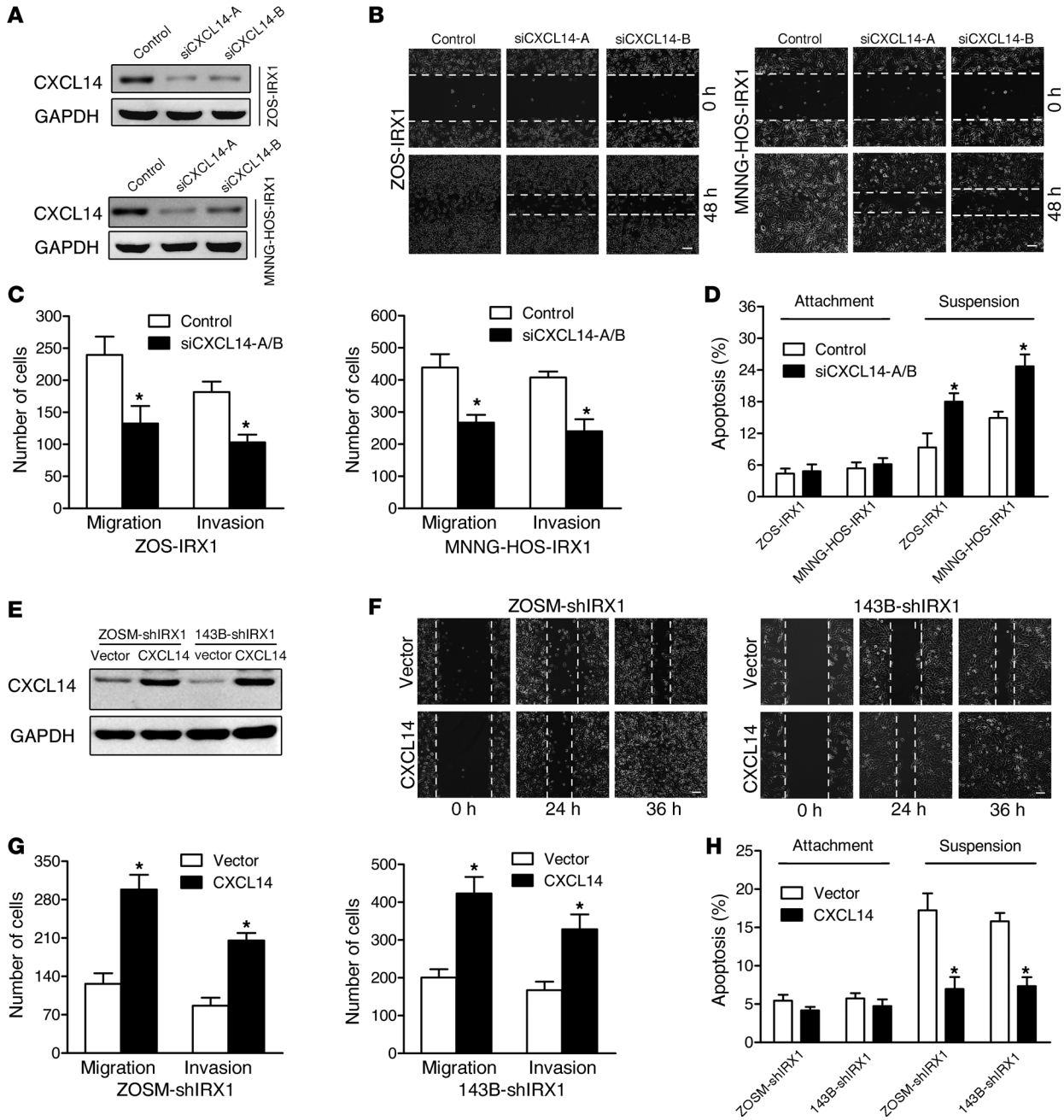

Figure 7. IRX1 promotes osteosarcoma progression through CXCL14. (**A**) The effect of CXCL14 siRNA was confirmed by Western blot analysis. (**B**) CXCL14 knockdown dramatically reduced the migratory ability of *IRX1*-overexpressing cells. (**C**) Downregulation of CXCL14 reduced the migratory and invasive abilities of IRX1-overexpressing cells. (**D**) Knockdown of CXCL14 promoted apoptosis in IRX1-overexpressing nonadherent cells but had no effect on attached cells. (**E**) The efficiency of CXCL14 overexpression in ZOSM-IRX1 and 143B-IRX1 cells was confirmed by Western blot analysis. (**F**) CXCL14 overexpression increased the migratory ability of IRX1-depleted ZOSM and 143B cells. (**G**) CXCL14 overexpression enhanced the migratory and invasive abilities of IRX-1-depleted ZOSM and 143B cells. (**H**) Overexpression of CXCL14 significantly inhibited cell death under nonadherent culture conditions. Scale bars: 100 μm. Data represent the mean ± SD of 3 separate determinations. $^*P < 0.05$ by Student's *t* test.

Because IRX1 is a transcription factor, we examined whether IRX1 upregulated CXCL14 by activating the *CXCL14* promoter. A human *CXCL14* promoter fragment (nucleotides –2000 to +515) was cloned into the pGL3 luciferase vector and then cotransfected with an shRNA targeting IRX1 into 143B cells or with an *IRX1* cDNA construct into MNNG-HOS cells. IRX1 knockdown clearly suppressed *CXCL14* promoter activity in the 143B-shIRX1 cells, while IRX1 overexpression in the MNNG-HOS cells enhanced *CXCL14* promoter activity (Figure 5G). Further inspection of the *CXCL14* promoter revealed 2 predicted IRX1-binding sites (26): site A at –857 bp (ACACCTGT) and site B at –1950 bp (ACATCTGT). The presence of these sites suggests that IRX1 might directly activate CXCL14 expression. We then examined whether IRX1 could bind to the *CXCL14* promoter in the context

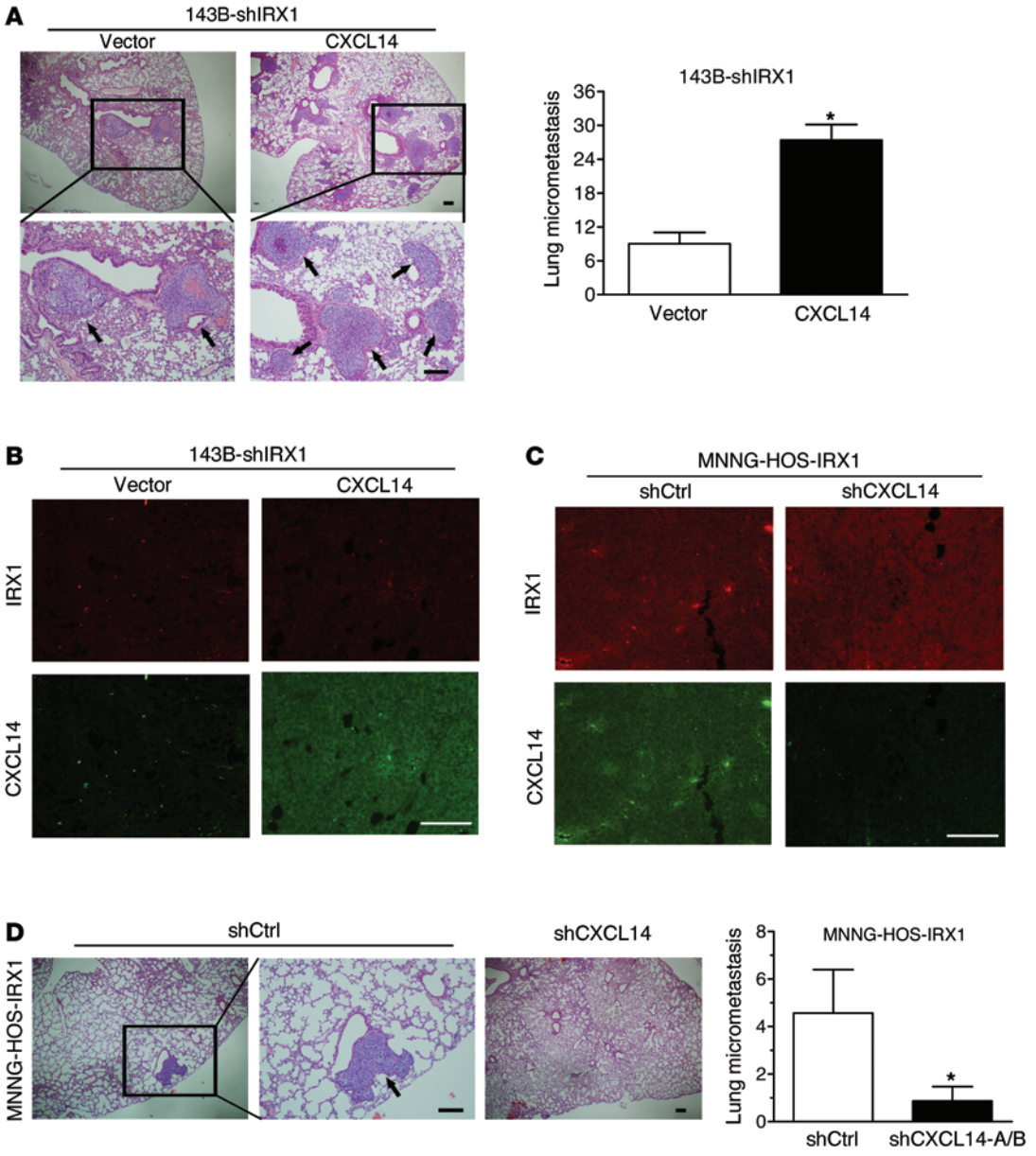

Figure 8. IRX1 promotes lung metastasis through CXCL14 in a mouse model. (**A**) CXCL14 overexpression significantly enhanced the metastatic ability of IRX1-knockdown 143B cells. (**B**) Immunofluorescence analysis of IRX1 and CXCL14 in tumors from 143B cell–bearing mice. (**C**) Immunofluorescence analysis of IRX1 and CXCL14 expression in tumors from MNNG-HOS cell–bearing mice. (**D**) CXCL14 knockdown in MNNG-HOS-IRX1 cells significantly decreased lung metastases. Black arrow indicates the metastatic nodule. Scale bars: 200 μm (**A** and **D**), 100 μm (**B** and **C**). *$P < 0.05$ by Student's *t* test.

of chromatin. ChIP analysis revealed that IRX1 could bind to site A on the *CXCL14* promoter (Figure 5H); however, PCR with primers that flanked site B did not produce a detectable product when IRX1-immunoprecipitated DNA was used as a template. Taken together, these results indicate that IRX can bind specific DNA sequences (ACACCTGT) in the *CXCL14* promoter and directly activate *CXCL14* transcription.

IRX1/CXCL14 signaling is required for lung metastasis of osteosarcoma cells. Given that CXCL14 can promote the invasion of pancreatic and breast cancer cells and is associated with the metastasis of colorectal cancer (15, 17, 18), we next determined whether CXCL14 could also promote metastatic phenotypes in osteosarcoma cells. Our results demonstrated that transfection of ZOS cells with a CXCL14 expression vector promoted migration, invasion, and resistance to anoikis (Figure 6, A and B). Given that CXCL14 is a secreted protein, we used a neutralizing antibody to block CXCL14. CXCL14 blockade in the culture medium attenuated the metastasis-promoting effects of CXCL14 overexpression on ZOS cells (Figure 6, A and B). Conversely, transfection of ZOSM cells with CXCL14 siRNA significantly inhibited metastatic behaviors, and recombinant CXCL14 reversed the effect of CXCL14 suppression in ZOSM cells (Figure 6, C and D). In addition, ZOS cells treated with conditioned medium from ZOSM control, but not ZOSM-siCXCL14, cells enhanced cell migration, invasion, and resistance to anoikis (Figure 6, E and F). Similar results were obtained when MNNG-HOS and 143B cells

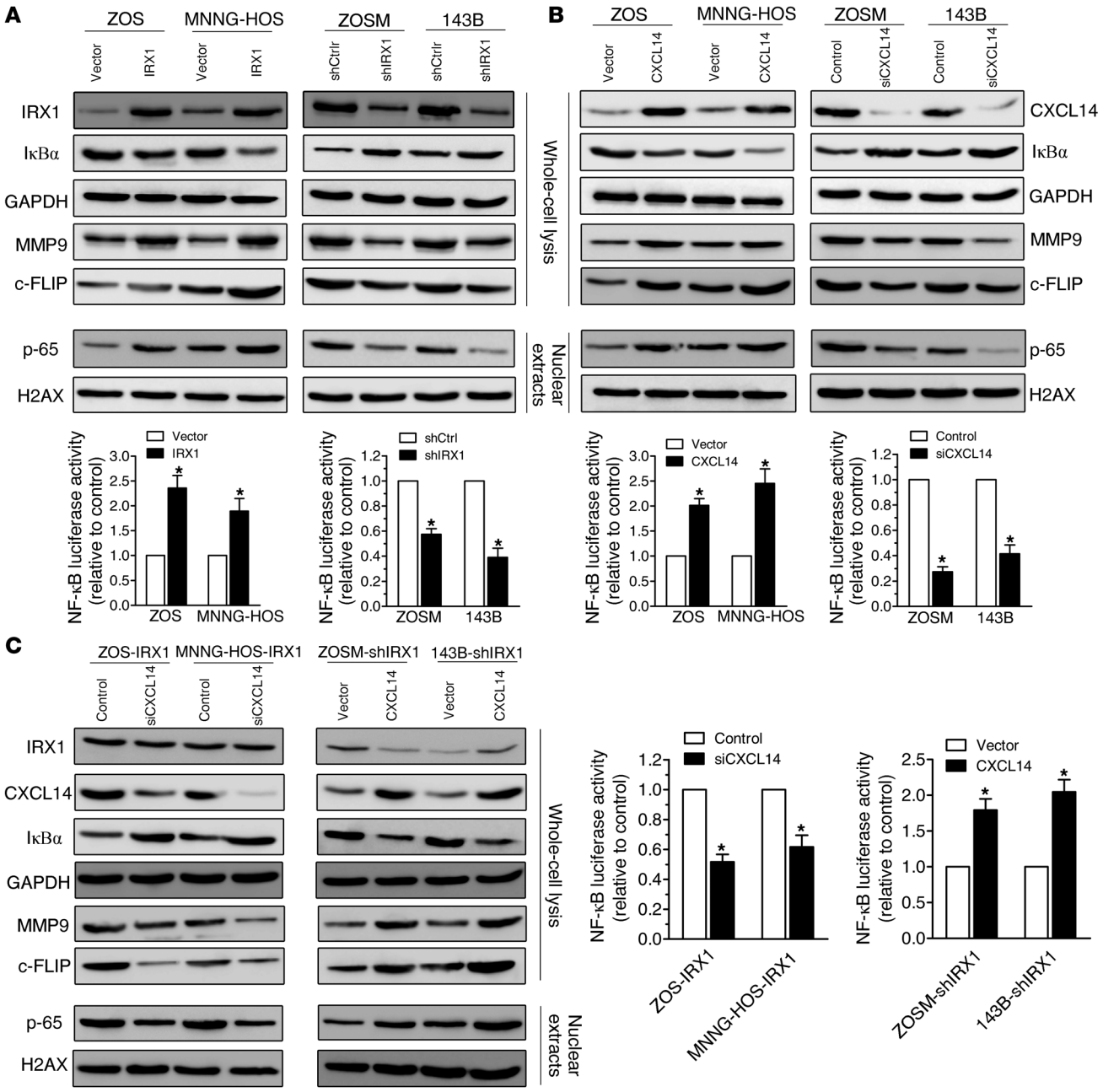

Figure 9. IRX1 activates NF-κB signaling through CXCL14. (**A**) Western blot analysis was performed to detect production of the indicated proteins in control and IRX1-overexpressing or -knockdown osteosarcoma cells. An NF-κB luciferase reporter assay was performed on the indicated cells. (**B**) Expression of the indicated proteins was determined in control and CXCL14-overexpressing or in CXCL14-knockdown osteosarcoma cells. An NF-κB luciferase reporter assay was performed on the indicated cells. (**C**) Expression of the indicated proteins and NF-κB luciferase reporter activity were determined in the indicated cells. Data represent the mean ± SD of 3 separate determinations. **P* < 0.05 by Student's *t* test.

were used (Supplemental Figure 6). These results showed that CXCL14 could promote the metastatic behavior of osteosarcoma cells and that it likely acts in an autocrine fashion.

We then asked whether CXCL14 participates in IRX1-mediated lung metastasis. First, we examined the effect of CXCL14 impairment on IRX1 function. In proliferation assays, the siRNA-mediated downregulation of CXCL14 in ZOS-IRX1 and MNNG-HOS-IRX1 cells had no significant effects on cell growth when compared with control cells (Supplemental Figure 7A). However, wound-healing and Transwell assays showed that CXCL14 knockdown in ZOS-IRX1 and MNNG-HOS-IRX1 cells resulted in a decrease in their migratory and invasive abilities (Figure 7, A–C). Transfection with CXCL14 siRNA also reduced anoikis resistance in ZOS and MNNG-HOS cells overexpressing IRX1 (Figure 7D). Furthermore, CXCL14 blockade in the culture medium with a neutralizing antibody could inhibit the migration, invasion, and resistance to anoikis of ZOS-IRX1 and MNNG-HOS-IRX1 cells as effectively as CXCL14 siRNA (Supplemental Figure 8). These

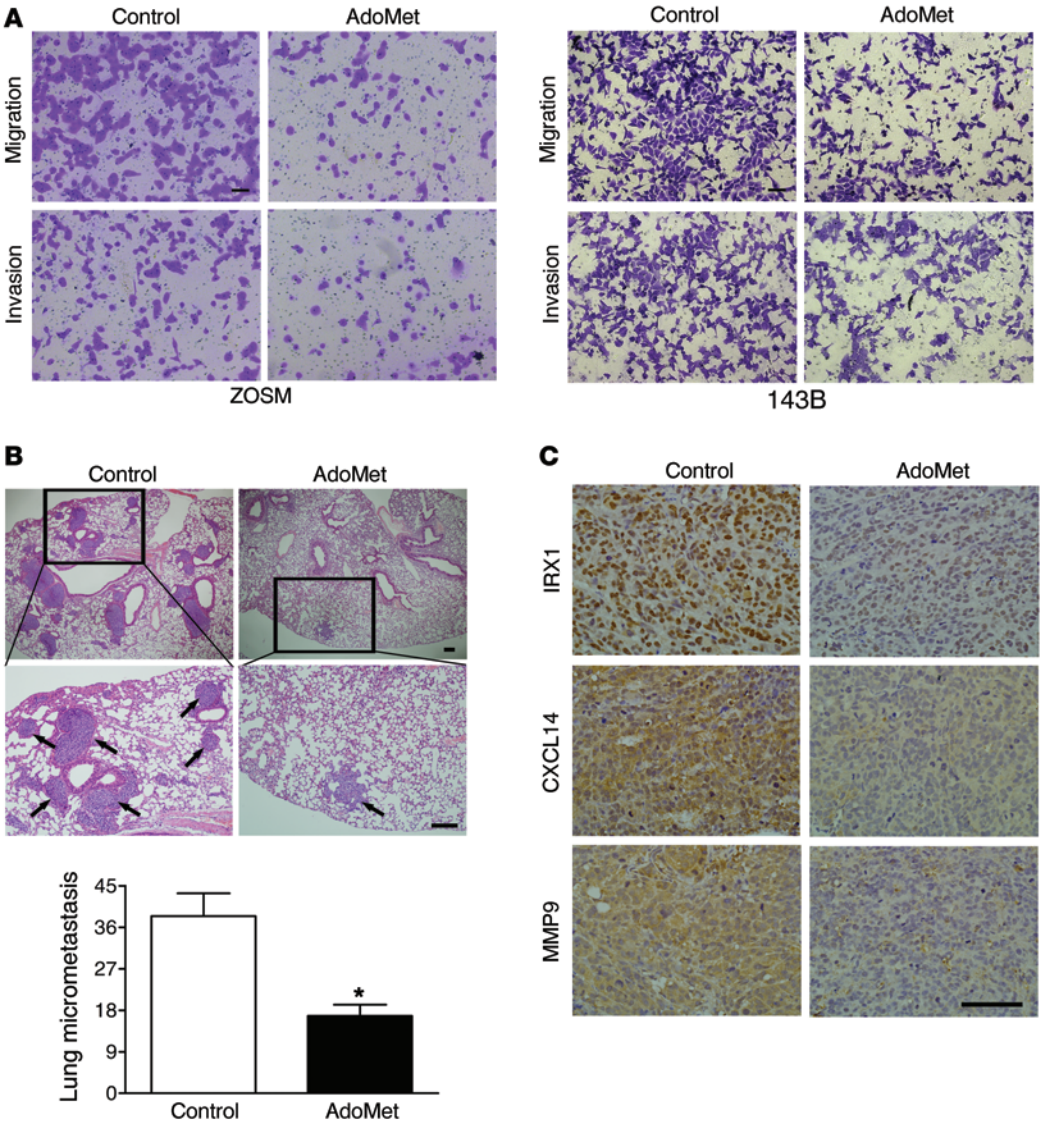

Figure 10. AdoMet inhibits the metastasis of osteosarcoma cells. (**A**) A Transwell assay showed that the migratory and invasive abilities of ZOSM and 143B cells were significantly suppressed after treatment with 500 μM AdoMet for 6 days. (**B**) 143B cells with control or AdoMet treatment (500 μM) were injected into the proximal tibia of NOD/SCID mice (n = 10), and the rate of lung metastasis was measured by histopathological analysis at 5 weeks. AdoMet treatment dramatically decreased the number of lung micrometastases. (**C**) Immunohistochemical analysis of IRX1, CXCL14, and MMP9 expression in tumors from mice that received control or AdoMet-treated 143B cells. Scale bars: 100 μm (**A** and **C**), 200 μm (**B**). *$P < 0.05$ by Student's t test.

findings suggest that IRX1 promotes osteosarcoma progression through the autocrine action of CXCL14.

To investigate whether CXCL14 overexpression can compensate for the loss of IRX1 function, a *CXCL14* cDNA expression construct was transiently transfected into ZOSM-shIRX1-A and 143B-shIRX1-A cells. Overexpression of CXCL14 increased migration, invasion, and resistance to anoikis in IRX1-knockdown ZOSM and 143B cells without impacting cell growth (Figure 7, E–H, and Supplemental Figure 7B), further confirming that CXCL14 is required for the prometastatic activity of IRX1 in osteosarcoma cells.

Next, we determined whether CXCL14 could reverse the metastatic ability of IRX1-knockdown cells in vivo. First, 143B–shIRX1-A cells were transfected with *CXCL14* cDNA or an empty vector and inoculated into NOD/SCID mice. CXCL14 overexpression in 143B-shIRX1 cells promoted metastasis to the lung, and the decrease in metastatic activity caused by *IRX1* deletion was abolished (Figure 8, A and B). To further confirm the effect of CXCL14 on IRX1-induced osteosarcoma metastasis, mice were injected with CXCL14 shRNA– or control shRNA–transfected MNNG-HOS-IRX1 cells. Compared with the control cells, lung metastases of the MNNG-HOS-IRX1 cells were suppressed after CXCL14 knockdown (Figure 8, C and D). Along with our earlier observations, these findings indicate that IRX1 promotes osteosarcoma cell metastasis in vivo through upregulated CXCL14 expression.

NF-κB pathway activation is involved in IRX1/CXCL14-induced signaling osteosarcoma metastasis. We next explored the underlying mechanisms of how IRX1/CXCL14 signaling influences the metastatic phenotypes of osteosarcoma cells. It has been demonstrated that CXCL14 enhances the invasiveness of pancreatic cancer cells by increasing NF-κB transactivation (17). Our previous studies showed that activation of NF-κB could promote the progression of osteosarcoma (27, 28), which suggests that the effect of IRX1/CXCL14 signaling on osteosarcoma cells involves the NF-κB pathway. Therefore, we aimed to determine whether IRX1 and CXCL14 overexpression promotes osteosarcoma metastasis by activating the NF-κB pathway.

To do so, we initially examined the influence of IRX1 on NF-κB signaling. Our results showed that overexpression of IRX1 in ZOS and MNNG-HOS cells increased the degradation of IκBα, the

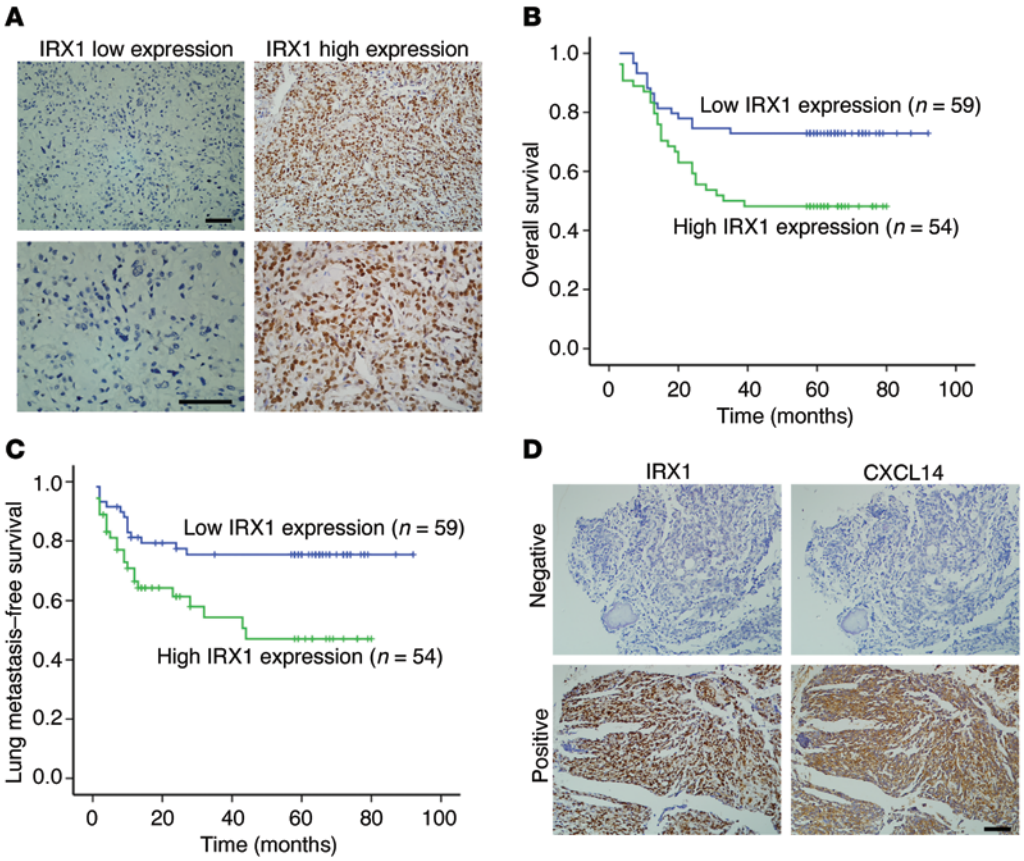

Figure 11. Clinical relevance of IRX1 and CXCL14 expression in human osteosarcoma specimens. (**A**) Immunohistochemical staining was used to detect IRX1 protein expression in osteosarcoma tissues (n = 113). Representative images of low and high IRX1 expression are shown. Scale bars: 100 μm. (**B**) Overall survival was significantly higher in the low-IRX1-expression group (log-rank test, P = 0.011). (**C**) The risk of lung metastasis was significantly higher in the high-IRX1-expression group (log-rank test, P = 0.009). (**D**) Representative positive and negative staining of IRX1 and CXCL14 in human osteosarcoma tissue sections. Scale bar: 100 μm.

nuclear translocation of NF-κB p65, and NF-κB luciferase reporter activity (Figure 9A). In addition, the protein levels of NF-κB target genes, such as matrix metallopeptidase 9 (*MMP9*) and cellular FLICE-inhibitory protein (*c-FLIP*), which are involved in cancer cell invasion and anoikis resistance (29–31), were increased following IRX1 overexpression. In contrast, IRX1 knockdown in ZOSM and 143B cells significantly decreased NF-κB p65 nuclear translocation, NF-κB-luciferase reporter activity, and expression of MMP9 and c-FLIP (Figure 9A).

We next investigated whether CXCL14 overexpression or knockdown could affect NF-κB activity. Transfection of ZOS and MNNG-HOS cells with a CXCL14 expression vector enhanced the nuclear translocation of NF-κB p65 and increased NF-κB luciferase reporter activity (Figure 9B). Furthermore, transfection of ZOSM and 143 cells with CXCL14 siRNA significantly decreased CXCL14 protein levels, and cells with reduced CXCL14 expression showed lower nuclear NF-κB p65 expression and lower NF-κB luciferase reporter activity compared with control cells (Figure 9B). Although the functional relationship between CXCL14 and NF-κB activation is not yet understood, these observations suggest that NF-κB activation is a consequence of CXCL14 upregulation in osteosarcoma cells.

We then examined whether CXCL14 was essential for IRX-1-induced NF-κB activation. CXCL14 expression was suppressed by siRNA in ZOS-IRX1 and MNNG-HOS-IRX1 cells, and NF-κB activity was then measured. CXCL14 siRNA markedly reduced nuclear NF-κB levels and NF-κB luciferase reporter activity in ZOS-IRX1 and MNNG-HOS-IRX1 cells (Figure 9C). When a CXCL14 expression vector was transiently transfected into ZOSM-shIRX1 or 143B-shIRX1 cells, both nuclear NF-κB expression and NF-κB–luciferase reporter activity were completely rescued in the IRX1-deficient cells (Figure 9C), suggesting that CXCL14 is required for IRX1-induced NF-κB activation. Taken together, our findings indicate that IRX1 can activate NF-κB signaling via CXCL14 upregulation.

Finally, we determined whether blocking the NF-κB pathway using the NF-κB inhibitor BAY 11-7085, which inhibits the phosphorylation and degradation of IκBα and prevents the translocation of p65/p50 (32), attenuated the metastasis-promoting effect of IRX1- and CXCL14-overexpressing osteosarcoma cells. As shown in Supplemental Figure 9, the metastatic ability of ZOS-IRX1 and MNNG-HOS-IRX1 cells was significantly suppressed after BAY 11-7085 treatment (2.5 μM). These results indicate that NF-κB pathway activation is involved in IRX1/CXCL14-induced metastasis in osteosarcoma cells.

The DNA-methylating drug AdoMet inhibits osteosarcoma metastasis. We have shown above that AdoMet could methylate the promoter of *IRX1* and hence suppress IRX1 expression in ZOSM and 143B cells (Figure 2, F and G). We thus investigated whether AdoMet could also inhibit osteosarcoma metastasis. ZOSM and 143B cells were treated with 500 μM AdoMet for 6 days prior to performing a Transwell assay. As shown in Figure 10A, AdoMet treatment decreased the migratory and invasive abilities of ZOSM and 143B cells. However, there was no significant difference in detachment-induced apoptosis after AdoMet treatment (Supplemental Figure 10A). We next examined the

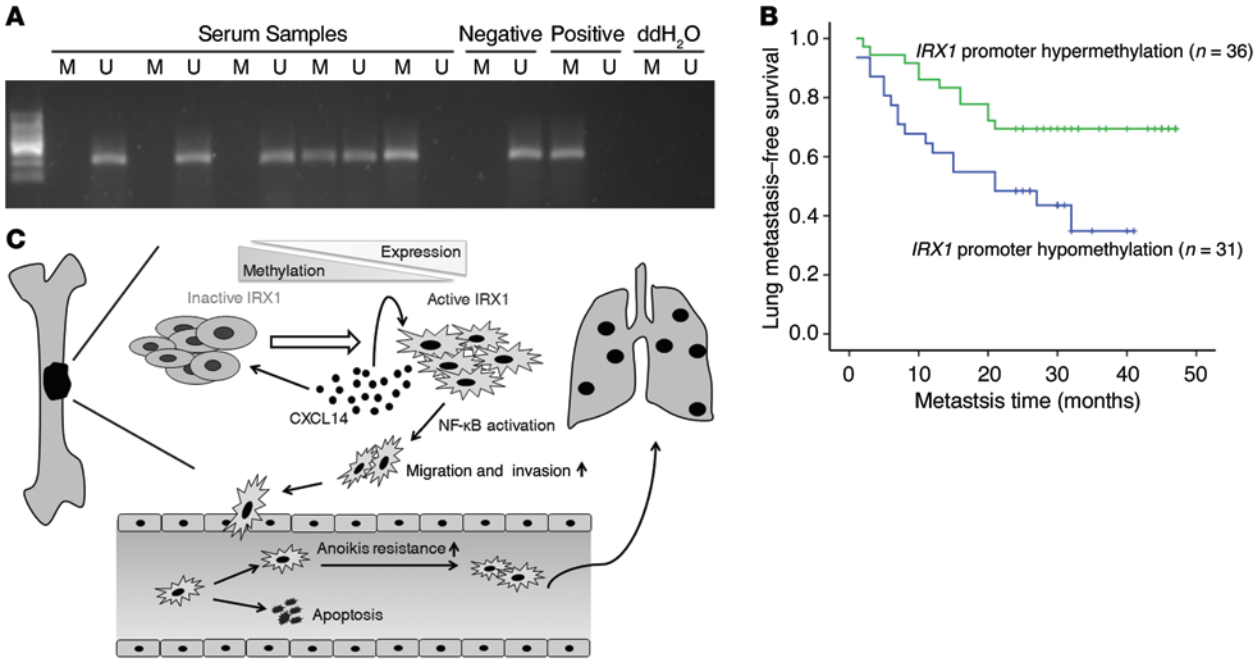

Figure 12. Prognostic relevance of *IRX1* promoter methylation in serum DNA from osteosarcoma patients. (**A**) Methylation-specific PCR analysis of the *IRX1* promoter region in the serum DNA of osteosarcoma patients (n = 67). M, hypermethylated *IRX1*; U, unmethylated *IRX1*. Representative images of serum samples, including negative and positive controls. (**B**) Patients with hypomethylation of the *IRX1* promoter in their serum DNA had a lower rate of lung metastasis–free survival (log-rank test, P = 0.014). (**C**) Potential mechanism by which IRX1 promotes osteosarcoma metastasis. IRX1 is activated by hypomethylation of its own promoter as osteosarcoma progresses. Overexpression of IRX1 leads to increased autocrine activity of CXCL14 and promotes metastatic behavior of osteosarcoma cells via NF-κB activation.

effect of AdoMet on the metastatic ability of osteosarcoma cells in vivo. AdoMet-treated and control 143B cells were injected into the proximal tibiae of NOD/SCID mice (n = 10 per group), and lungs were checked for metastasis at 5 weeks. The results of the examination demonstrated that mice inoculated with AdoMet-treated 143B cells developed significantly fewer metastatic tumor foci in their lungs than did control mice (Figure 10B). We then determined whether in vitro treatment with AdoMet resulted in stable silencing of IRX1 expression in tumors in vivo. Immunohistochemical staining showed strong positive expression of IRX1 in the tumors from the control group (Figure 10C). In contrast, weak staining for IRX1 was observed in the tumors formed from the AdoMet-treated cells. Furthermore, the expression levels of CXCL14 and MMP9 were also reduced in the tumors from the AdoMet-treated group. These findings suggested that the DNA-methylating drug AdoMet inhibited osteosarcoma metastasis in part through reversing hypomethylation of the *IRX1* promoter and suppressing IRX1 expression.

We also examined the influence of the demethylating drug DAC, which has been demonstrated to increase IRX1 expression in ZOS and MNNG-HOS cells, on the metastatic behaviors of osteosarcoma cells. Our results showed that ZOS and MNNG-HOS cells treated with 2 μM DAC for 3 days exhibited greater migratory and invasive abilities in vitro than did control cells (Supplemental Figure 10, B and C). Nevertheless, DAC-treated ZOS and MNNG-HOS cells were more sensitive to detachment-induced apoptosis than were control cells (Supplemental Figure 10D), and there was no significant difference in lung metastasis in vivo after DAC treatment of MNNG-HOS cells (data not shown).

Prognostic value of IRX1 in human osteosarcoma patients. On the basis of our demonstration that IRX1 is prometastatic in osteosarcoma, we evaluated the clinical significance of IRX1 in primary human osteosarcoma specimens. To this end, surgical specimens from 113 cases of osteosarcoma, collected between January 2004 and December 2008, were examined for IRX1 expression by immunohistochemical staining (Supplemental Table 3). As shown in Figure 11A, IRX1 staining was mainly observed in the nuclei of tumor cells. The correlations between IRX1 expression and other clinical characteristics are presented in Supplemental Table 4. Kaplan-Meier survival analysis indicated that patients with high IRX1 expression levels had worse overall survival than did those with low expression levels (Figure 11B). Moreover, the risk of lung metastases was significantly higher in the patients expressing high levels of IRX1 than in those expressing low levels of the protein (Figure 11C). Multivariate analyses revealed that high IRX1 expression was an independent predictor of poor prognosis and lung metastasis (Supplemental Table 5).

Given that IRX1 requires CXCL14 to induce metastasis, we further examined whether there was a positive correlation between IRX1 and CXCL14 protein expression in human osteosarcoma tissues. Immunohistochemical staining for CXCL14 was performed in the same cohort of 113 patients with osteosarcoma (Supplemental Table 3). CXCL14 staining in osteosarcoma cells was mainly located in the cytoplasm (Figure 11D). χ^2 analysis indicated that there was a significant correlation between the pres-

Table 1. Immunohistochemical staining of IRX1 and CXCL14 in 113 osteosarcoma tissues

	CXCL14	IRX1	
Staining		+	–
No. (%)	+	39 (34.5%)	27 (23.9%)
	–	15 (13.3%)	32 (28.3%)

$P = 0.004$ by χ^2 test.

ence of nuclear IRX1 and cytoplasmic CXCL14 (Table 1), which further confirmed that CXCL14 was essential for the prometastatic effects of IRX1 in osteosarcoma.

IRX1 promoter hypomethylation in patient serum DNA predicts the lung metastasis of osteosarcoma. Compared with tumor tissue–based biomarkers, circulating blood biomarkers are easily available and less invasive. It has been demonstrated that epigenetic changes in cell-free tumor DNA can be detected in the serum of cancer patients (33, 34). To determine whether hypomethylation of *IRX1* in serum DNA is a potential marker for lung metastasis of osteosarcoma, we examined the methylation status of the *IRX1* promoter by methylation-specific PCR (MSP) in 67 serum samples collected from primary osteosarcoma patients between August 2010 and September 2012. Representative results of MSP for the *IRX1* promoter are shown in Figure 12A. There was no association between *IRX1* promoter methylation in the serum DNA and patient age, sex, tumor site, or Enneking stage (Table 2). However, we found that the *IRX1* promoter was hypomethylated in 34.2% of serum samples (13 of 38) from patients without metastases, while 62.1% of serum samples (18 of 29) from the metastatic group showed *IRX1* promoter hypomethylation ($P = 0.023$, χ^2 test). Kaplan-Meier analysis indicated that patients with hypomethylated *IRX1* in their serum exhibited worse lung metastasis–free survival than did those with hypermethylation (Figure 12B), suggesting that the detection of *IRX1* promoter hypomethylation in the serum DNA of osteosarcoma patients could be a potential predictive marker for monitoring lung metastasis in osteosarcoma.

Discussion

Cancer metastasis is a complex process that involves several molecular and cellular changes, among which aberrant epigenetic alteration is now widely recognized as one of the most important events (35–37). In this study, we identified *IRX1* as a hypomethylation-activated metastasis-driving gene in osteosarcoma. Suppression of IRX1 decreased CXCL14 expression levels and NF-κB activity and had antimetastatic effects in mouse models of osteosarcoma. We conclude that hypomethylation-mediated activation of IRX1 positively regulates CXCL14/NF-κB signaling to promote metastatic activities in osteosarcoma and that therapeutic targeting of the IRX1 pathway may be a promising strategy for suppressing osteosarcoma metastasis.

The Iroquois transcription factor family, which plays multiple roles in many metazoan developmental processes (5, 8), has recently been shown to be involved in the development of many cancers (6, 38–41). For example, IRX3 downregulation in breast cancer was linked to poor clinical outcomes, and IRX4 expression suppressed prostate cancer growth (39, 41). IRX1 was reported to be downregulated in HNSCC and gastric cancer, and it inhibited cancer cell growth, invasion, and tumorigenesis. (6, 7). However, we show here that *IRX1* is overexpressed in metastatic osteosarcoma and that it functions as a prometastatic gene, suggesting that IRX1 might play dual roles in cancer development. In fact, there are many genes like *IRX1* that have been demonstrated to play both tumor-suppressing and tumor-promoting roles that depend on the cancer type (42, 43). For instance, insulin-like growth factor–binding protein 5 (IGFBP5) has been shown to induce apoptosis and inhibit tumor growth in breast cancer and osteosarcoma cells (44, 45). In contrast, IGFBP5 was found to facilitate the progression of prostate cancer (46). Nevertheless, the reasons for the contradicting functions of IRX1 in different tissue contexts are unclear. It has been reported that Iroquois transcription factors may have context-dependent dual functions as activators and repressors (47). Indeed, IRX2 can be converted from a repressor to an activator after being phosphorylated by FGF8/MAPK signaling (48). In gastric cancer, IRX1 was identified as a transcriptional repressor that could downregulate the expression of a set of tumor-promoting genes such as *BDKRB2*, *FGF7*, and *HIST2H2BE* and thereby inhibit angiogenesis, cell proliferation, and invasion (6). We also found in the present study that IRX1 acted as a transcriptional activator to promote the expression of prometastatic genes like *CXCL14* to facilitate osteosarcoma metastasis. Switching of IRX1 between transcriptional activation and repression may contribute to its distinct roles in different types of cancer. However, the molecular basis of such switching requires further investigation. Importantly, antimetastatic strategies that target IRX1 signaling

Table 2. Association of *IRX1* promoter methylation in serum DNA with the clinicopathological characteristics of 48 osteosarcoma patients

	U[A]	M[B]	*P* value[C]
Sex			0.664
Female	13	17	
Male	18	19	
Age (yr)			0.110
≤20	18	27	
21–40	10	9	
>40	3	0	
Location			0.430
Distal femur	20	21	
Proximal tibia	4	8	
Proximal femur	5	7	
Proximal humerus	2	0	
Enneking stage			0.674
IIA	1	3	
IIB	24	26	
III	6	7	
Metastasis			0.023
No	13	25	
Yes	18	11	

[A]U, hypomethylation; [B]M, hypermethylation; [C]χ^2 test.

must consider its dual roles in cancer and must include specific targeting of therapeutic agents to avoid increasing the risk of other cancers such as HNSCC and gastric cancer.

A large body of evidence has demonstrated that chemokines play key roles in several critical steps during the metastatic process, including migration, invasion, extravasation, and angiogenesis (49–51). Here, we identified *CXCL14*, a novel CXC chemokine, as a potential target gene of IRX1 by using a high-throughput screening method. CXCL14 has also been found to be upregulated in several cancer types and is associated with tumor progression and metastasis (15, 17–19). Consistent with these findings, we showed that CXCL14 enhanced the metastatic ability of osteosarcoma cells in an autocrine manner. Furthermore, IRX1 was able to induce CXCL14 expression by directly binding to its promoter. CXCL14 knockdown attenuated IRX1-induced metastasis in osteosarcoma, while CXCL14 overexpression partially compensated for the loss of IRX1 function. Our observations indicate that CXCL14 is a bona fide downstream effector of IRX1 in osteosarcoma metastasis. However, CXCL14 is a relatively new chemokine whose receptor is unknown and whose function is undefined, thus making it difficult to identify a pathway through which CXCL14 promotes cancer metastasis. Given that CXCL14 belongs to a chemokine family that is involved in inflammatory processes (52) and given that NF-κB signaling plays an important role in the control of inflammatory response (53), it seems reasonable that CXCL14 may activate that NF-κB pathway. In fact, it has been recently demonstrated that CXCL14 can increase nuclear NF-κB p65 levels and promote the invasiveness of pancreatic cancer cells (17). In the present study, we found that IRX1/CXCL14 signaling could activate the NF-κB pathway and increase the expression of MMP9 and c-FLIP, thus promoting osteosarcoma metastasis. Together with our earlier findings (27, 28), these results indicate that the NF-κB pathway acts as a key node in the signaling networks regulating osteosarcoma progression.

DNA methylation, a DNA modification that occurs via the covalent addition of a methyl group to cytosine by DNA methyltransferases (DNMTs), is an important epigenetic mechanism that regulates gene expression (54, 55). Recent studies have provided compelling evidence that aberrant DNA methylation plays a pivotal role in cancer initiation and progression (2, 56, 57). However, the majority of studies have focused on hypermethylation of the promoter CpG islands of tumor-suppressor genes. The impact of hypomethylation, especially the loss of promoter methylation, has been underestimated (58). In this report, we demonstrated that elevated expression of the prometastatic gene *IRX1* was associated with hypomethylation of the *IRX1* promoter and that DNA demethylation may be a major cause of IRX1 activation in osteosarcoma (Figure 2, A–F). This may explain why the IRX1 expression pattern in osteosarcoma is different from that observed in HNSCC and gastric cancers, in which *IRX1* is silenced by promoter hypermethylation (6, 7). Given that DNA methylation is a reversible process, the pharmacological inhibition of demethylation may result in inhibition of the expression of prometastatic genes (such as *IRX1*) as well as metastasis (59). AdoMet, a ubiquitous methyl donor in the DNA methyltransferase reaction, is a safe and natural compound that has been used for the treatment of depression, liver disease, and osteoarthritis (60–62). Recent studies have shown that it can increase DNA methylation by either stimulating DNA methyltransferase activity or by inhibiting demethylation activity (23). Importantly, AdoMet was able to suppress *uPA* and *MMP2* expression by reversing the hypomethylation status of their promoters, thereby blocking the associated breast and prostate cancer metastases (63, 64). Consistent with this finding, we showed that AdoMet treatment could also cause methylation of the *IRX1* promoter and decrease *IRX1* gene expression (Figure 2, G–I). Moreover, treatment with AdoMet suppressed the migratory and invasive abilities of osteosarcoma cells in vitro and their metastatic potential in vivo. Given that AdoMet is a broadly acting methylating drug, it may also induce hypermethylation of many other metastasis-related genes in addition to *IRX1*. Further studies are required to determine the mechanism through which AdoMet inhibits the invasiveness and metastasis of osteosarcoma cells. Nevertheless, one concern with using methylating drugs is that they may cause hypermethylation of tumor-suppressor genes and thereby promote tumorigenesis. It is therefore not recommended that methylating drugs be used at early stages of cancer, when tumor-suppressor genes may be easily silenced by hypermethylation (63). Thus, it is important to develop methylating drugs that are more potent and specific than AdoMet. On the other hand, it must be noted that, although the demethylating drug DAC showed no significant effect on metastasis in the in vivo mouse model studied here, use of DAC might indeed activate prometastatic genes (such as *IRX1*) and promote the invasiveness of osteosarcoma cells. Taken together, our observations not only indicate that reversion of hypomethylation may provide a new strategy for the effective control of osteosarcoma metastasis, but also warn against using demethylating drugs in the late stages of cancer therapy.

The molecular detection of epigenetic changes in cell-free tumor DNA in serum has been highlighted as a potential tool for cancer diagnosis and prognosis (65). Here, we used highly sensitive MSP to detect the *IRX1* promoter methylation status using cell-free tumor DNA obtained from the serum of osteosarcoma patients. We found that the *IRX1* promoter was hypomethylated in 46.3% (31 of 67) of serum samples and that patients with *IRX*1 promoter hypomethylation in their serum DNA were more likely to have lung metastasis. Given that aberrant gene methylation is one of the earliest molecular changes that occurs during cancer progression (66, 67), the detection of *IRX1* hypomethylation in serum DNA could be a promising strategy for the early detection of osteosarcoma lung metastasis and might be useful for guiding individual treatment and assessing the early response to chemotherapy.

In summary, our present study identified hypomethylated *IRX1* as a metastasis-driving gene that promotes osteosarcoma lung metastasis by enhancing CXCL14/NF-κB signaling (Figure 12C). Because the methylation process is reversible, the pharmacologic reversion of hypomethylation-activated IRX1 may be a novel option for the prevention of osteosarcoma metastasis.

Methods

Microarray analysis. The MeDIP assay was performed using the Human DNA Methylation 3×720K CpG Island Plus RefSeq Pro-

moter Array (NimbleGen), and the data were deposited in the NCBI's Gene Expression Omnibus (GEO) database (GEO GSE55961). Gene expression microarray analysis was performed using the Affymetrix Human Genome U133 Plus 2.0 Array (ZOS vs. ZOSM) and the NimbleGen Human Gene Expression 12×135K Array (143B-shCtrl vs. 143B-shIRX1), and the microarray data were deposited in the GEO database (GEO GSE55957 and GSE55958). Further details are provided in the Supplemental Methods.

Animal studies. Four- to six-week-old female NOD/SCID mice were purchased from Beijing HFK Bioscience Co. Ltd. Mice were injected with 2×10^6 cells (in 100 μl PBS) into the lateral tail vein (10 mice per group). The mice were monitored 3 times per week for evidence of morbidity associated with pulmonary metastases. After 8 weeks, the mice were sacrificed by cervical dislocation. Subsequently, the lungs were harvested, fixed in 4% paraformaldehyde, and embedded in paraffin. For the orthotopic model of osteosarcoma, mice were anesthetized with 4% chloral hydrate (0.2 ml/100 g, i.p.). The right knee of the mouse was flexed beyond 90°, and 1×10^6 cells suspended in 30 μl PBS were injected into the right proximal tibia using a 30-gauge needle (10 mice per group). The tumor volume was measured in 2 perpendicular dimensions (D1, D2) with an electronic digital caliper every 3 days and calculated using the formula: $V = 4/3\pi[1/4(D1 + D2)]^2$, as described previously (68). After 5 weeks, the mice were anesthetized, and bone destruction caused by the tumor was observed using the Inveon Micro-CT/PET system (Siemens). The mice were then sacrificed, and the lungs were harvested, fixed in 4% paraformaldehyde, and embedded in paraffin. To quantify the number of pulmonary metastatic lesions, sequential serial 3-μm-thick sections of whole lungs were obtained. The sections were stained with H&E to identify the metastases by light microscopy as previously described (69).

Experimental procedures. See the Supplemental Methods for details on other experimental procedures. All primers used in this study are listed in Supplemental Table 6.

Statistics. Statistical analyses were performed using SPSS software, version 16.0 (SPSS Inc.). Measurements were analyzed using the 2-tailed Student's *t* test, the Mann-Whitney *U* test, or 1-way ANOVA, while categorical data were analyzed with the χ^2 or Fisher's exact test. Correlations between the relative expression levels of IRX1 and CXCL14 were analyzed using Pearson's correlation method. Associations between *IRX1* promoter methylation and gene expression were determined by the Spearman's rank correlation test. Survival curves were calculated using the Kaplan-Meier method, and differences were analyzed with the log-rank test. The Cox regression model was used for multivariate survival analysis. A *P* value of less than 0.05 was considered statistically significant.

Study approval. This study was approved by the ethics committee of Sun Yat-Sen University, and written informed consent was obtained from the patients or their guardians before sample collection. All animal studies were approved by the IACUC of Sun Yat-Sen University.

Acknowledgments

This research was supported by the National Natural Science Foundation of China (81272940 and 81472507, to Jin Wang and 81001194, to Changye Zou); a Talent Grant from Sun Yat-Sen University (13yk2d08, to Jin Wang); the PhD Program Foundation of the Ministry of Education of China (20130171110062, to Jin Wang); and the Sun Yat-Sen University Clinical Research 5010 Program (2012002, to Jin Wang). We thank J. Zhao (Sun Yat-Sen University) for expert technical assistance.

Address correspondence to: Jin Wang, Jingnan Shen, or Huiling Yang, Department of Musculoskeletal Oncology, The First Affiliated Hospital of Sun Yat-Sen University, No. 58, Zhongshan Road 2, Guangzhou, Guangdong, China 510080. Phone: 8620.87755766-8236; E-mail: 2004wjhf@163.com.

1. Siegel HJ, Pressey JG. Current concepts on the surgical and medical management of osteosarcoma. *Expert Rev Anticancer Ther*. 2008;8(8):1257–1269.
2. Esteller M. Epigenetics in cancer. *N Engl J Med*. 2008;358(11):1148–1159.
3. Al-Romaih K, Sadikovic B, Yoshimoto M, Wang Y, Zielenska M, Squire JA. Decitabine-induced demethylation of 5′ CpG island in GADD45A leads to apoptosis in osteosarcoma cells. *Neoplasia*. 2008;10(5):471.
4. Al-Romaih K, et al. Modulation by decitabine of gene expression and growth of osteosarcoma U2OS cells in vitro and in xenografts: Identification of apoptotic genes as targets for demethylation. *Cancer Cell Int*. 2007;7(1):14.
5. Cavodeassi F, Modolell J, Gómez-Skarmeta JL. The Iroquois family of genes: from body building to neural patterning. *Development*. 2001;128(15):2847–2855.
6. Guo X, et al. Homeobox gene IRX1 is a tumor suppressor gene in gastric carcinoma. *Oncogene*. 2010;29(27):3908–3920.
7. Bennett KL, et al. Frequently methylated tumor suppressor genes in head and neck squamous cell carcinoma. *Cancer Res*. 2008;68(12):4494–4499.
8. Zulch A, Becker MB, Gruss P. Expression pattern of Irx1 and Irx2 during mouse digit development. *Mech Dev*. 2001;106(1-2):159–162.
9. Miller NH, et al. Linkage analysis of genetic loci for kyphoscoliosis on chromosomes 5p13, 13q13.3, and 13q32. *Am J Med Genet A*. 2006;140(10):1059–1068.
10. Selvarajah S, et al. Identification of cryptic microaberrations in osteosarcoma by high-definition oligonucleotide array comparative genomic hybridization. *Cancer Genet Cytogenet*. 2007;179(1):52–61.
11. Hromas R, et al. Cloning of BRAK, a novel divergent CXC chemokine preferentially expressed in normal versus malignant cells. *Biochem Biophys Res Commun*. 1999;255(3):703–706.
12. Frederick MJ, et al. In Vivo Expression of the Novel CXC Chemokine BRAK in Normal and Cancerous Human Tissue. *Am J Pathol*. 2000;156(6):1937–1950.
13. Schwarze SR, Luo J, Isaacs WB, Jarrard DF. Modulation of CXCL14 (BRAK) expression in prostate cancer. *Prostate*. 2005;64(1):67–74.
14. Ozawa S, Kato Y, Komori R, Maehata Y, Kubota E, Hata R. BRAK/CXCL14 expression suppresses tumor growth in vivo in human oral carcinoma cells. *Biochem Biophys Res Commun*. 2006;348(2):406–412.
15. Allinen M, et al. Molecular characterization of the tumor microenvironment in breast cancer. *Cancer Cell*. 2004;6(1):17–32.
16. Oler G, Camacho CP, Hojaij FC, Michaluart P, Riggins GJ, Cerutti JM. Gene expression profiling of papillary thyroid carcinoma identifies transcripts correlated with BRAF mutational status and lymph node metastasis. *Clin Cancer Res*. 2008;14(15):4735–4742.
17. Wente MN, et al. CXCL14 expression and potential function in pancreatic cancer. *Cancer Lett*. 2008;259(2):209–217.
18. Zeng J, et al. Chemokine CXCL14 is associated with prognosis in patients with colorectal carcinoma after curative resection. *J Transl Med*. 2013;11(1):6.
19. Lu J, et al. [Expression of chemokine CXCL14 in primary osteosarcoma and its association with prognosis]. *Nan Fang Yi Ke Da Xue Xue Bao*. 2013;33(6):798–803.
20. Zou CY, et al. Establishment and characteristics of two syngeneic human osteosarcoma cell lines from primary tumor and skip metastases. *Acta Pharmacol Sin*. 2008;29(3):325–332.
21. Tan P, et al. Expression and prognostic relevance of PRAME in primary osteosarcoma. *Biochem Biophys Res Commun*. 2012;419(4):801–808.

22. Luu HH, et al. An orthotopic model of human osteosarcoma growth and spontaneous pulmonary metastasis. *Clin Exp Metastasis*. 2005;22(4):319–329.
23. Detich N, Hamm S, Just G, Knox JD, Szyf M. The methyl donor S-Adenosylmethionine inhibits active demethylation of DNA: a candidate novel mechanism for the pharmacological effects of S-Adenosylmethionine. *J Biol Chem*. 2003;278(23):20812–20820.
24. Simpson CD, Anyiwe K, Schimmer AD. Anoikis resistance and tumor metastasis. *Cancer Lett*. 2008;272(2):177–185.
25. Kim YN, Koo KH, Sung JY, Yun UJ, Kim H. Anoikis resistance: an essential prerequisite for tumor metastasis. *Int J Cell Biol*. 2012;2012:306879.
26. Bilioni A, Craig G, Hill C, McNeill H. Iroquois transcription factors recognize a unique motif to mediate transcriptional repression in vivo. *Proc Natl Acad Sci U S A*. 2005;102(41):14671–14676.
27. Zhao Z, et al. Downregulation of MCT1 inhibits tumor growth, metastasis and enhances chemotherapeutic efficacy in osteosarcoma through regulation of the NF-kappaB pathway. *Cancer Lett*. 2014;342(1):150–158.
28. Tang QL, et al. Glycogen synthase kinase-3beta, NF-kappaB signaling, and tumorigenesis of human osteosarcoma. *J Natl Cancer Inst*. 2012;104(10):749–763.
29. Safa AR. c-FLIP, a master anti-apoptotic regulator. *Exp Oncol*. 2012;34(3):176–184.
30. Micheau O, Lens S, Gaide O, Alevizopoulos K, Tschopp J. NF-kappaB signals induce the expression of c-FLIP. *Mol Cell Biol*. 2001;21(16):5299–5305.
31. Park SH, Riley Pt, Frisch SM. Regulation of anoikis by deleted in breast cancer-1 (DBC1) through NF-kappaB. *Apoptosis*. 2013; 18(8):949–962.
32. Pierce JW, et al. Novel inhibitors of cytokine-induced IkappaBalpha phosphorylation and endothelial cell adhesion molecule expression show anti-inflammatory effects in vivo. *J Biol Chem*. 1997;272(34):21096–21103.
33. Schwarzenbach H, Hoon DS, Pantel K. Cell-free nucleic acids as biomarkers in cancer patients. *Nat Rev Cancer*. 2011;11(6):426–437.
34. Müller HM, Fiegl H, Widschwendter A, Widschwendter M. Prognostic DNA methylation marker in serum of cancer patients. *Ann N Y Acad Sci*. 2004;1022(1):44–49.
35. Gupta GP, Massagué J. Cancer metastasis: building a framework. *Cell*. 2006;127(4):679–695.
36. Nguyen DX, Massagué J. Genetic determinants of cancer metastasis. *Nat Rev Genet*. 2007;8(5):341–352.
37. Rodenhiser DI. Epigenetic contributions to cancer metastasis. *Clin Exp Metastasis*. 2009;26(1):5–18.
38. Adamowicz M, et al. Frequent amplifications and abundant expression of TRIO, NKD2, and IRX2 in soft tissue sarcomas. *Genes Chromosomes Cancer*. 2006;45(9):829–838.
39. Asaka S, Fujimoto T, Akaishi J, Ogawa K, Onda M. Genetic prognostic index influences patient outcome for node-positive breast cancer. *Surg Today*. 2006;36(9):793–801.
40. Myrthue A, et al. The iroquois homeobox gene 5 is regulated by 1,25-dihydroxyvitamin D3 in human prostate cancer and regulates apoptosis and the cell cycle in LNCaP prostate cancer cells. *Clin Cancer Res*. 2008;14(11):3562–3570.
41. Nguyen HH, et al. IRX4 at 5p15 suppresses prostate cancer growth through the interaction with vitamin D receptor, conferring prostate cancer susceptibility. *Hum Mol Genet*. 2012;21(9):2076–2085.
42. Bosch-Presegue L, Vaquero A. The dual role of sirtuins in cancer. *Genes Cancer*. 2011;2(6):648–662.
43. Robbs BK, Cruz AL, Werneck MB, Mognol GP, Viola JP. Dual roles for NFAT transcription factor genes as oncogenes and tumor suppressors. *Mol Cell Biol*. 2008;28(23):7168–7181.
44. Su Y, et al. Insulin-like growth factor binding protein 5 suppresses tumor growth and metastasis of human osteosarcoma. *Oncogene*. 2011;30(37):3907–3917.
45. Butt AJ, Dickson KA, McDougall F, Baxter RC. Insulin-like growth factor-binding protein-5 inhibits the growth of human breast cancer cells in vitro and in vivo. *J Biol Chem*. 2003;278(32):29676–29685.
46. Xu C, et al. Regulation of global gene expression in the bone marrow microenvironment by androgen: androgen ablation increases insulin-like growth factor binding protein-5 expression. *Prostate*. 2007;67(15):1621–1629.
47. Itoh M, Kudoh T, Dedekian M, Kim CH, Chitnis AB. A role for iro1 and iro7 in the establishment of an anteroposterior compartment of the ectoderm adjacent to the midbrain-hindbrain boundary. *Development*. 2002;129(10):2317–2327.
48. Matsumoto K, et al. The prepattern transcription factor Irx2, a target of the FGF8/MAP kinase cascade, is involved in cerebellum formation. *Nat Neurosci*. 2004;7(6):605–612.
49. Balkwill F. Cancer and the chemokine network. *Nat Rev Cancer*. 2004;4(7):540–550.
50. Sun X, et al. CXCL12 / CXCR4 / CXCR7 chemokine axis and cancer progression. *Cancer Metastasis Rev*. 2010;29(4):709–722.
51. Balkwill FR. The chemokine system and cancer. *J Pathol*. 2012;226(2):148–157.
52. Pelicano H, et al. Mitochondrial dysfunction and reactive oxygen species imbalance promote breast cancer cell motility through a CXCL14-mediated mechanism. *Cancer Res*. 2009;69(6):2375–2383.
53. O'Dea E, Hoffmann A. NF-kappaB signaling. *Wiley Interdiscip Rev Syst Biol Med*. 2009;1(1):107–115.
54. Razin A, Riggs AD. DNA methylation and gene function. *Science*. 1980;210(4470):604–610.
55. Razin A, Cedar H. DNA methylation and gene expression. *Microbiol Rev*. 1991;55(3):451–458.
56. Wajed SA, Laird PW, DeMeester TR. DNA methylation: an alternative pathway to cancer. *Ann Surg*. 2001;234(1):10–20.
57. Ehrlich M. DNA methylation in cancer: too much, but also too little. *Oncogene*. 2002;21(35):5400–5413.
58. Ehrlich M. DNA hypomethylation in cancer cells. *Epigenomics*. 2009;1(2):239–259.
59. Egger G, Liang G, Aparicio A, Jones PA. Epigenetics in human disease and prospects for epigenetic therapy. *Nature*. 2004;429(6990):457–463.
60. Delle Chiaie R, Pancheri P, Scapicchio P. Efficacy and tolerability of oral and intramuscular S-adenosyl-L-methionine 1, 4-butanedisulfonate (SAMe) in the treatment of major depression: comparison with imipramine in 2 multicenter studies. *Am J Clin Nutr*. 2002;76(5):1172S–1176S.
61. Najm WI, Reinsch S, Hoehler F, Tobis JS, Harvey PW. S-adenosyl methionine (SAMe) versus celecoxib for the treatment of osteoarthritis symptoms: a double-blind cross-over trial. [ISRCTN36233495]. *BMC Musculoskelet Disord*. 2004;5(1):6.
62. Mato JM, Lu SC. Role of S-adenosyl-L-methionine in liver health and injury. *Hepatology*. 2007;45(5):1306–1312.
63. Pakneshan P, Szyf M, Farias-Eisner R, Rabbani SA. Reversal of the hypomethylation status of urokinase (uPA) promoter blocks breast cancer growth and metastasis. *J Biol Chem*. 2004;279(30):31735–31744.
64. Shukeir N, Pakneshan P, Chen G, Szyf M, Rabbani SA. Alteration of the methylation status of tumor-promoting genes decreases prostate cancer cell invasiveness and tumorigenesis in vitro and in vivo. *Cancer Res*. 2006;66(18):9202–9210.
65. Alix-Panabieres C, Schwarzenbach H, Pantel K. Circulating tumor cells and circulating tumor DNA. *Annu Rev Med*. 2012;63:199–215.
66. Sidransky D. Emerging molecular markers of cancer. *Nat Rev Cancer*. 2002;2(3):210–219.
67. Laird PW. The power and the promise of DNA methylation markers. *Nat Rev Cancer*. 2003;3(4):253–266.
68. Tang QL, et al. Salinomycin inhibits osteosarcoma by targeting its tumor stem cells. *Cancer Lett*. 2011;311(1):113–121.
69. Su Y, et al. Establishment and characterization of a new highly metastatic human osteosarcoma cell line. *Clin Exp Metastasis*. 2009;26(7):599–610.